Gas modulated Fabry-Perot-cavity-based refractometry (GAMOR) — Guide to its basic features, performance, and implementation

Report on the A1.4.3 activity in task 1.4 (Gas Modulation Methodologies) in the EMPIR project 18SIB04, "QuantumPascal"

Isak Silander[1], Johan Zakrisson[1], Clayton Forssén[1,2], Martin Zelan[2], and Ove Axner[1]

[1]**Department of Physics, Umeå University, SE-901 87 Umeå, Sweden**
[2]**Measurement Science and Technology, RISE Research Institutes of Sweden, SE-501 15 Borås, Sweden**

Abstract Although Fabry-Perot-cavity (FPC) based refractometry has demonstrated an extraordinary potential for assessment of refractivity and pressure, such systems are often adversely affected by various type of disturbances (drifts, fluctuations, and noise). The realization of high-performance systems therefore requires an exceptional mechanical stability, a low noise electrical environment, and temperature stabilized conditions. The gas modulation refractometry (GAMOR) methodology has been developed to automatically mitigate the influence of various types of disturbances on assessments of refractivity. It is based on two principles: (*i*) an assessment of the refractivity of the gas in the measurement cavity by a frequent referencing of filled measurement cavity beat frequencies to evacuated cavity beat frequencies; and (*ii*) an estimate of the empty measurement cavity beat frequency by an interpolation between two evacuated beat frequency assessments performed just before and after the filled cavity assessments. By this, the methodology can swiftly mitigate the influence of various types of disturbances in refractometry systems, e.g. changes in length of the cavity caused by relaxations or drifts in the temperature of the spacer and drifts from gas leakages and outgassing. The methodology has demonstrated an outstanding performance regarding precision; it has repeatedly demonstrated assessments with sub parts-per-million precision. This guide provides a compilation of the principles, properties, and performance of the GAMOR methodology applied to dual FPC (DFPC) refractometry. First, a short introduction to ordinary FPC-based refractometry is given, where its susceptibility to various types of disturbances is highlighted. The guide then provides general expressions for how to assess refractivity from measurements of shifts of the beat frequency and mode hops that serve as the basis for FPC-based refractometry in general as well as for GAMOR based instrumentation. Pressure is then assessed by the use of the Lorentz-Lorenz expression and an equation of state. This is followed by explanations and descriptions of the ability of the GAMOR methodology to mitigate the influence of fluctuations and drifts. Next, a short description of the most commonly used experimental set-up, viz. an Invar-based DFPC system, is given. This is followed by an illustration of the operation and performance of the methodology. A summary of the most important achievements of the GAMOR methodology is given. After an experimental verification of the ability of the GAMOR methodology to mitigate the influence of fluctuations and drifts, its precision is illustrated under various conditions. It is shown that an Invar-based FPC system can provide a sub-0.1 ppm precision when addressing vacuum pressures and that two GAMOR based refractomomters coupled to the same pressure gauge can provide a short-term correlation that is well into the 10^{-8} range. It is also shown that these properties have allowed for the development of disturbance-resistant methodologies for assessment of cavity deformation and mirrors penetration depth. To assess its uncertainty, also the influence of pV-work and its ability to assess the gas temperature have been addressed. It has been concluded that GAMOR-based instrumentation can provide an expanded uncertainty (k=2) of $[(10\ \text{mPa})^2 + (10 \times 10^{-6}P)^2]^{1/2}$. It is also shown that its extraordinary properties allows for realization of transportable set-ups. Finally, to facilitate the dissemination of the GAMOR methodology, this guide provides a recipe on how to implement GAMOR in a DFPC-system.

Contents

1 Introduction **4**
- 1.1 The pascal . . . 4
- 1.2 Fabry–Perot-based refractometry . . . 4

2 Limitations of refractometry **5**
- 2.1 Definition of various types of disturbances and their origin . . . 5
- 2.2 Conventional means to reduce the influence of disturbances in refractometry . . . 5
- 2.3 A novel means to reduce the influence of disturbances on the assessment of refractivity — Gas Modulation Refractometry (GAMOR) . . . 6
- 2.4 Content of this guide . . . 6

3 Theory **7**
- 3.1 Assessment of refractivity . . . 7
  - 3.1.1 General expression for the refractivity assessed from a single FP cavity in the presence of cavity deformation, mirror penetration depth, and the Gouy phase . . . 7
  - 3.1.2 Dual-FP-cavity refractometry . . . 9
  - 3.1.3 Procedures and expressions for the GAMOR methodology . . . 9
  - 3.1.4 A note on the uncertainty in assessments of refractivity . . . 10
- 3.2 Molar Density . . . 11
- 3.3 Pressure . . . 11
- 3.4 Molecular Data . . . 11

4 Theoretical analysis and explication of the ability of the GAMOR methodology to automatically mitigate the influence of disturbances **11**
- 4.1 Ability of the GAMOR methodology to mitigate the influence of fluctuations . . . 12
- 4.2 Ability of the GAMOR methodology to mitigate the influence of drifts . . . 14
  - 4.2.1 Qualitative description . . . 14
  - 4.2.2 Quantitative analysis . . . 15

5 Experimental Setup **16**
- 5.1 GAMOR instrumentation - General realization . . . 16
- 5.2 The Invar-based DFPC system . . . 17
  - 5.2.1 The refractometry system . . . 17
  - 5.2.2 The gas handling system . . . 18

6 A cycle-resolved illustration of the operation and performance of the GAMOR methodology **18**

7 Achievements of GAMOR **20**
- 7.1 Experimental verification of the predicted abilities of the GAMOR methodology to mitigate the influence of disturbances . . . 21
  - 7.1.1 Verification of the predicted ability of GAMOR to reduce the influence of fluctuations . . . 21
  - 7.1.2 Verification of the predicted ability of GAMOR to reduce the influence of drifts . . . 22
- 7.2 Demonstration of the ability of the GAMOR methodology to improve on precision . . . 23
  - 7.2.1 Ability of GAMOR to reduce the influence of drifts from a non-temperature stabilized system . . . 23
  - 7.2.2 An alternative realization of GAMOR— Gas-equilibration GAMOR (GEq-GAMOR) . . . 23
  - 7.2.3 Assessment of precision of the Invar-based DFPC system utilizing the GAMOR methodology . . . 24

7.2.4 Short-term performance of two Invar-based DFPC GAMOR systems for assessment of pressure . . . 27
7.3 Demonstration of the ability of GAMOR-based refractometer systems to provide low uncertainty assessments . . . 28
7.3.1 The influence of thermodynamic effects (***pV***-work) on the assessments and the ability to assess gas temperature accurately . . . 28
7.3.2 Development of a Ga fixed-temperature cell for accurate assessment of temperature. . 29
7.3.3 Development of a disturbance-resistant methodology for assessment of cavity deformation 29
7.3.4 Development of a methodology for accurate in-situ assessment of the penetration depth of mirrors comprising a quarter-wave stack (QWS) high-reflection coating of type H . . 30
7.3.5 Assessment of the uncertainty of the stationary and the transportable Invar-based FPC optical Pascals — the SOP and the TOP — for assessment of pressure . . . 30
7.4 Realization of transportable refractometer systems based on the GAMOR methodology . . . 31

8 A summary of the basic features of the GAMOR methodology 32

9 A recipe on how to construct a GAMOR-based FPC refractometry system suitable for high precision and low uncertainty assessments 33

1 Introduction

1.1 The pascal

In the SI-system of units, the pascal is defined as the force per unit area. In practice, it is realized with mechanical devices such as pressure balances and liquid manometers [1–5]. Their performance, however, has remained essentially unchanged over the past few decades and they suffer from practical and environmental limitations.

By the revision of the SI-system 2019 in which the Boltzmann constant was given a fixed value [6, 7] and by highly accurate ab-initio calculations that relate optical properties of the gas to its number density (e.g., the molar polarisability of helium has been calculated with an uncertainty of 10^{-7} [8]), an alternative path to realize the pascal has become feasible [9]. By measuring the refractivity and the temperature of a gas, it is possible to calculate its pressure by the use of the Lorentz–Lorenz equation and an equation of state [10–17].

Since such an assessment of pressure is not dependent on any mechanical actuator but instead measures directly on the gas, it potentially decreases uncertainties and shortens calibration chains. This justifies the use of optical techniques for assessment of pressure and realization of the pascal.

1.2 Fabry–Perot-based refractometry

The most sensitive instruments are currently based on Fabry–Perot (FP) cavities (FPCs) where a laser is used to probe the frequency of a longitudinal mode [13–22].

FPC-based refractometry is built on the fact that the index of refraction, n, constitutes the ratio of an optical length in the presence and absence of gas; for FPC-based refractometry, with and without gas in the cavity, here referred to as L ($= nL_0$) and L_0, respectively [13–17]. In practice, the optical lengths are assessed by measuring the frequency of a laser that is locked to a longitudinal mode of the cavity. By this, the shift of the frequency of the mode that takes place when gas is let into an FPC will be transferred to a shift in the frequency of the laser light.[1]

Since frequency is the entity that can be assessed with highest accuracy in our society (up to one part in 10^{16} and potentially even one part in 10^{18}) [23–25], where the basic limitation is thermal noise in the mirror substrate and coatings, and the cavity spacer, this opens up extraordinary abilities regarding precision and dynamic range. While assessments of pressure with a single instrumentation today are commonplace from the low mPa region up to atmospheric pressure (100 kPa), it has been prophesied that both µPa and hundreds of kPa assessments might soon also be prevalent [9, 16–18, 26–29]. Much of this was the basis for the EMPIR JRP 18SIB04 "QuantumPascal" project that was initiated 2019. At the start of this project, the then most advanced optical realisation of the pascal, based on a dual FPC (DFPC) interferometer at NIST (the FLOC system), had demonstrated a claimed relative uncertainty of 9×10^{-6} at 100 kPa and 2×10^{-3} at 1 Pa [30].

Although that work demonstrated the extraordinary potential of FPC-based interferometry, as is further discussed below, it has unfortunately also been recognized that FPC-based refractometry systems are highly sensitive to various types of disturbances. The realization of high-performance systems therefore requires an exceptional mechanical stability and a quiet (i.e. a noise-, interference-, and drift-minimized) environment. However, some of the actions performed to achieve such conditions have been found to cause various types of limitations. For example, ultra-low expansion (ULE) glass, which has been used to reach ultra-stable conditions [17, 30], has shown to have a permeability of He that gives rise to significant memory effects in the form of reduced gas purity, increased residual gas pressure, and altered cavity length [31], which has aggravated low uncertainty assessments. Attempts to alleviate such effects have included means to let the cavity relax for a substantial amount of time, which though instead introduces drifts. Issues such as these have, for some time, limited the use of FP-refractometry for accurate assessments of pressure and realization of the pascal.

As a means to mitigate this type of limitations, the gas modulation refractometry (GAMOR) methodology, which has an ability to minimize (or

[1] A common way to assess such a shift is to mix the frequency of the laser light down to a radio frequency (RF) by the use of another laser (a reference laser). This can practically be achieved by merging the two laser fields onto a photodiode. By this, the beat frequency between the two can be measured directly from the photodiode response by the use of a frequency counter. This implies that the shift in the frequency of the cavity mode addressed when gas is let into the cavity is converted to a shift into a measured beat frequency.

even eliminate) the influence of several of these types of limitations, has been developed. This guide provides a compilation of the principles, properties, and performance of the GAMOR methodology followed by a detailed recipe on how to implement GAMOR in a DFPC-system

2 Limitations of refractometry

2.1 Definition of various types of disturbances and their origin

Hence, although it is simple in theory to realize FPC-based instrumentation and to perform low uncertainty refractivity assessments, it is not trivial in practice to carry them out. One reason is that FPCs often are exposed to a variety of disturbances on different time scales, for simplicity here referred to as[2]

- high-frequency disturbance ($f \geq 0.1$ Hz), here denoted *noise*;
- low-frequency periodic disturbances ($10\ \mu\text{Hz} \leq f \leq 0.1$ Hz), referred to as *fluctuations*; and
- monotonic (or ultra-low frequency) disturbances ($f \leq 10\ \mu$Hz), termed *drifts*.

While noise can originate from a number of sources, e.g. electronics, fast vibrations, and turbulence, fluctuations can be caused by slow air pressure variations, slow vibrations (e.g. from motions of air damped optical tables or buildings), slow disturbances of the central supply of power, and temperature regulation processes in electronics. Drifts can originate from a number of sources, not least from changes of the length of the cavity, e.g. from thermal expansion, aging, relaxations, and diffusion of gas into the material that can change its length in an unpredicted manner. Irrespective of whether the disturbances can be identified or not, all of them will affect the ability to perform high quality (high precision and low uncertainty) measurements, sometimes severely [15, 17, 31–33].

The high sensitivity to disturbances was early recognized as a practical limitation of FPC-based interferometry for high-accuracy assessment of pressure and realization of the pascal. For example, a disturbance that causes a change in the length the cavity of 1 pm, a fraction of the "size" of an individual atom, gives rise to, for a 15 cm long cavity, a change in pressure of 2 mPa. It was therefore widely recognized that the realization of refractometry systems requires an exceptional mechanical stability.

This implies, among other things, that it is far from trivial to assess refractivity with low uncertainty by assessing L_0 and L in two separate assessments. A number of procedures to reduce the amount of disturbances, and thereby alleviate some of the above-mentioned limitations, have therefore, over the years, been developed and implemented.

2.2 Conventional means to reduce the influence of disturbances in refractometry

One means to reduce the amount of disturbances in a system is to base FPC-based refractometry on DFPCs in which the two cavities are simultaneously addressed by two laser fields and the change in mode frequency of the cavity in which gas is let in is assessed as the change in the beat frequency between the two cavities [16, 17, 27, 30, 31, 33–37]. An advantage of this is that any change in length of the spacer that affects both cavities similarly does not affect the assessment. However, since the lengths of two cavities also can fluctuate dissimilarly over time, DFPC-based refractometry will still be affected by disturbances, although often to a lesser extent [17].

Another means to alleviate the limitations are to construct the FPC of low thermal expansion glass, e.g., ULE glass [17, 30] or Zerodur [13–16, 18, 19, 33, 34, 36, 38–40], place it in a highly temperature stabilized environment (a combined gas and vacuum chamber) [17], and let the system relax and equilibrate for long time periods after each gas filling or emptying process [17]. However, several of these actions are cumbersome to pursue and increase both the complexity of the systems and the susceptibility to drifts. This limits the use of the technology outside well-controlled laboratories.

[2] There are no strict boarders between the various types of disturbances. We have here defined noise as periodic disturbances whose frequencies are above 0.1 Hz, since this corresponds to the inverse of the time over which consecutive data points typically are averaged, in this work denoted $1/t_{avg}$. Drifts are defined as monotonic disturbances or periodic disturbances whose frequencies are below the inverse of the time between the assessments of refractivity in the presence and absence of gas in conventional refractometry. Since this time is assumed to be in the order of 10^5 s, drifts are here defined as the disturbances whose frequencies are below 10 μHz. Fluctuations, finally, are characterized as disturbances whose frequencies are between these two.

Although these types of procedures frequently are utilized to reduce various types of disturbances, assessments of refractivity are still often limited by their residual amounts. This limits the performance and thereby the applicability of FPC-based refractometry, in particular when low pressures are assessed, since disturbances then can severely limit the sensitivity of the instrument.

2.3 A novel means to reduce the influence of disturbances on the assessment of refractivity — Gas Modulation Refractometry (GAMOR)

Instead of reducing the *amount* of disturbances in a system, it is alternatively possible to utilize a methodology that can reduce their *influence* on the assessment of refractivity. One such is gas modulation refractometry (GAMOR). This methodology is built upon two principles, here referred to as two cornerstones; viz.,

(i) the refractivity of the gas in the measurement cavity is assessed by a frequent referencing of filled measurement cavity beat frequencies to evacuated cavity beat frequencies; and

(ii) the evacuated measurement cavity beat frequency at the time of the assessment of the filled measurement cavity beat frequency is estimated by use of an interpolation between two evacuated measurement cavity beat frequency assessments, one performed directly before and one directly after the filled cavity assessments.

Molar density and pressure are then assessed from the refractivity as for "conventional" FP-based refractometry, i.e. by the use of the Lorentz-Lorenz expression and an equation of state.

By this, as is illustrated below, the GAMOR methodology mitigates swiftly and conveniently (i.e. automatically) the influence of various types of disturbances in refractometry systems, not only those from changes in length of the cavity (e.g. those caused by ageing or drifts in the temperature of the cavity spacer), but also several of those that have other origins (e.g. those from gas leakages and outgassing) [35, 41–44].

2.4 Content of this guide

This guide first provides (in section 3) expressions for assessment of refractivity in FPC-based refractometry in general, and in DFPC-based systems in particular, that are suitable for the GAMOR methodology. Focus is on FPC systems exposed to cavity deformation utilizing distributed Bragg reflector (DBR) equipped mirrors comprising a quarter wave stack (QWS) in which the outermost layer has the highest index of refraction, referred to as type H, in the presence of the Gouy phase.

It then describes (in section 4) the basic principles of the GAMOR methodology by separately providing explanations and descriptions of the ability of the GAMOR methodology to mitigate the influence of fluctuations and drifts.

It thereafter provides (in section 5) a short depiction of the most commonly used instrumentation for GAMOR-based refractometry, viz. an Invar-based DFPC system.

By use of some typical cycle-resolved data, it then gives (in section 6) an illustration of the operation and performance of the GAMOR methodology in practice.

Thereafter, it provides (in section 7) an overview of the most important and extraordinary achievements of the GAMOR methodology; in particular a verification of the theoretical predictions regarding its ability to mitigate the influence of fluctuations and drifts (in section 7.1) and an illustration of the extraordinary/exquisite precision it has achieved under various conditions (in section 7.2). After reporting on some concepts of importance for the ability of GAMOR-based refractometry performed in an Invar-based DFPC to provide low uncertainty assessments — its low susceptibility to thermodynamic effects, so called pV-work (in section 7.3.1), its ability to assess the gas temperature (in section 7.3.2), and its ability to accurately assess cavity deformation (in section 7.3.3) and penetration depth of mirrors comprising QWS coatings of type H (in section 7.3.4) — this guide reports (in section 7.3.5) on the extended uncertainty the methodology so far has achieved.

It then provides (in section 7.4) a demonstration of its ability to realize transportable FP-based refractometry systems.

Finally, after a summary of its basic features (in section 8), and most importantly, this guide provides (in section 9) a step-by-step recipe of how to realize the GAMOR methodology, both conceptually

(how to carry out the modulation and detection process) and practically (how to construct suitable instrumentation).

The guide is based upon scientific papers published during the last few years, to some extent dealing with the predecessor to the GAMOR methodology (Drift-free or Fast switching DFPC-based refractometry [33, 35, 36]), but mainly referring to papers addressing the GAMOR methodology, of which a few were published before the EMPIR JRP 18SIB04 "QuantumPascal" project [41–43] while a majority of them have been published as a part of it [44–58].

3 Theory

3.1 Assessment of refractivity

Irrespective of whether FPC-based refractometry is performed unmodulated or modulated, it is based on the same fundamental principle; it measures the change in refractivity between two situations, with and without gas in a cavity (henceforth referred to as the measurement cavity), as a change in the frequency of laser light that is locked to a mode of the cavity.

3.1.1 General expression for the refractivity assessed from a single FP cavity in the presence of cavity deformation, mirror penetration depth, and the Gouy phase

When the penetration depth from mirrors and the Gouy phase are taken into account, the frequency of a given mode in a Fabry-Perot (FP) cavity can be obtained by the use of a round-trip resonance condition for the phase of the light. As is shown in Appendix A, following Koks and van Exter [59], for the m^{th} TEM_{00} mode of an FP cavity with DBR mirrors, such a condition can be written as

$$2k_{in}(L_0+\delta L)+\phi_1+\phi_2-2\Theta_G=2\pi m, \qquad (1)$$

where k_{in} is the wave vector of the light in the cavity, L_0 the distance between the front facets of the two DBRs coatings of the mirrors when the cavity is empty, δL the pressure induced cavity deformation, ϕ_1 and ϕ_2 the reflection phases of the two DBR equipped mirrors, Θ_G the (single pass) Gouy phase, and m an integer, representing the number of the longitudinal mode the laser addresses, defined by Eq. (1).[3]

As is shown in Silander et al. [51] as well as in Appendix A, for the case with mirror coatings comprising a QWS of type H, and for the case when the working ranges are centred on the mirror center frequency, the frequency of the mode of the cavity the laser addresses in the absence and in the presence of gas (when addressing the m_0^{th} and the m^{th} modes, respectively), ν_0 and ν, can be written as

$$\nu_0=\frac{cm_0\left(1+\frac{\Theta_G}{\pi m_0}+\frac{\gamma_c}{m_0}\right)}{2\left(L_0+2L_{\tau,c}\right)} \qquad (2)$$

and

$$\nu=\frac{cm\left(1+\frac{\Theta_G}{\pi m}+\frac{n\gamma_c}{m}\right)}{2n\left(L_0+\delta L+2L_{\tau,c}\right)}, \qquad (3)$$

respectively, where we have introduced γ_c and $L_{\tau,c}$, two purely material-dependent but index-of-refraction-independent parameters, which, on the mirror center frequency, ν_c, are given by $2\tau_c\nu_c/n$ and $c\gamma_c/(4\nu_c)$, respectively, where τ_c is the group delay (GD), which represents the time delay a narrow-band light pulse experiences upon reflection.[4] For the case when an ideal QWS is considered, γ_c is given by $(n_H-n_L)^{-1}$, where the two indices of refraction denote the high and lower indices of the coating materials, respectively. It can be noticed that $L_{\tau,c}$ represents the frequency penetration depth of a single mirror ($2L_{\tau,c}$ thus represents the elongation of the length of the cavity experienced by the light during scans due to the penetration of light into the mirror coatings).

For sufficiently large changes in pressure in the cavity, the frequency of the laser cannot follow that of a given cavity mode, whereby it needs to make a

[3] When the effect of the mirror penetration depth and the Gouy phase are neglected, as has been the case in some situations when specific features of the technique have been under scrutiny [35, 41, 42, 52], it is customary to view the resonance condition as a condition on the number of wavelengths the light experiences under a round trip, as $2n(L_0+\delta L)=q\lambda$, where q is the number of wavelengths the light experiences in a round trip in the cavity.

[4] Equation (3) shows that when the mirror penetration depth and the Gouy phase are neglected, as was done in some previous works in which specific features of the technique were scrutinized (as, e.g., in [35, 41, 42, 52]), it is adequate to express the frequency of the cavity mode addressed in a simpler form, viz. as

$$\nu=\frac{cq}{2n(L_0+\delta L)}. \qquad (4)$$

mode jump. This implies that m might differ from m_0. Denoting this difference Δm, and, by defining the shift in the frequency of the laser that takes place when the gas is let into the cavity, $\Delta\nu$, as $\nu_0-\nu$, as is shown in the same Appendix as well as in Silander et al. [51], it is possible to express, when the working range is centered on the mirror center frequency, with a minimum of approximations (on the 10^{-9} to a low 10^{-8} level), the refractivity in term of measurable quantities and material parameters as

$$n-1=\frac{\frac{\Delta\nu}{\nu_0}(1+\frac{\Theta_G}{\pi m_0}+\frac{\gamma_c}{m_0})+\frac{\Delta m}{m_0}}{1-\frac{\Delta\nu}{\nu_0}(1+\frac{\Theta_G}{\pi m_0}+\frac{\gamma_c}{m_0})+\frac{\Theta_G}{\pi m_0}+n\varepsilon'}, \quad (5)$$

where we have introduced ε' as the refractivity-normalized relative elongation of the length of the cavity due to the presence of the gas, defined as $\frac{\delta L}{L'}\frac{1}{n-1}$, where L' is the length of the cavity mode addressed experienced by the light in vacuum, given by $L_0+2L_{\tau_c}$.[5,6]

Since the $n\varepsilon'$ product in the expression above has a weak dependence on refractivity, through both the n and the ε' entities, Eq. (5) constitutes an expression that has a weak recursivity.[7] However, as is shown in Silander et al. [51] as well as in Appendix A, when the relative elongation is assumed to be linear with pressure, i.e. when $\frac{\delta L}{L'}$ can be considered to be given by κP where P is the pressure of the gas and κ is the pressure-induced distortion coefficient, and when nitrogen is addressed, the weak dependencies of the n and the ε' entities cancel. In this case, Eq. (5) can be expressed in a simpler manner, without any recursivity, as

$$n-1=\frac{\frac{\Delta\nu}{\nu_0}(1+\frac{\Theta_G}{\pi m_0}+\frac{\gamma_c}{m_0})+\frac{\Delta m}{m_0}}{1-\frac{\Delta\nu}{\nu_0}(1+\frac{\Theta_G}{\pi m_0}+\frac{\gamma_c}{m_0})+\frac{\Theta_G}{\pi m_0}+\varepsilon_0'}, \quad (8)$$

where ε_0' is given by $\kappa RT\frac{2}{3A_R}$, where R, T, and A_R denote the ideal gas constant, the temperature, and the dynamic molar polarizability, respectively [41, 52].

Although Eq. (8) is fully adequate under the aforementioned conditions (i.e. when the relative elongation is linear with pressure and when nitrogen is addressed), and irrespective of whether any modulated methodology is used or not, it can, by defining an "effective" empty cavity frequency, ν_0', given by $\nu_0/(1+\frac{\Theta_G}{\pi m_0}+\frac{\gamma_c}{m_0})$, be written in a more succinct form, viz. as

$$n-1=\frac{\overline{\Delta\nu}+\overline{\Delta m}}{1-\overline{\Delta\nu}+\frac{\Theta_G}{\pi m_0}+\varepsilon_0'}, \quad (9)$$

where $\overline{\Delta\nu}$ is defined as $\Delta\nu/\nu_0'$ and where $\overline{\Delta m}$ is a short hand notation for $\frac{\Delta m}{m_0}$, that is more suitable when gas modulation, in which assessments often are performed in a real-time manner, is applied.

Since this expression has much resemblance with the previously used simpler type of expression, used when specific features of the technique were scrutinized [35, 41, 42] and when the influence of penetration depth and the Gouy phase were neglected, given by Eq. (7) in footnote 6 above, this shows that even when the penetration depth and the Gouy phase are taken into account, it is possible, with a few simple redefinitions of entities, to make use of the simpler type of expression.[8]

[5] It can be noticed that the deformation dependence of Eq. (5) agrees with that of Eq. (2) in Egan and Stone [16]; series expanding Eq. (5) in terms of the distortion ($n\varepsilon'$) and making use of the definition of ε' gives

$$n-1=\frac{\frac{\Delta\nu}{\nu_0}(1+\frac{\Theta_G}{\pi m_0}+\frac{\gamma_c}{m_0})+\frac{\Delta m}{m_0}}{1-\frac{\Delta\nu}{\nu_0}(1+\frac{\Theta_G}{\pi m_0}+\frac{\gamma_c}{m_0})+\frac{\Theta_G}{\pi m_0}}-n\frac{\delta L}{L_0'}. \quad (6)$$

This indicates that the ε'-concept is a fully analogous alternative to the $\frac{\delta L}{L_0'}$-concept to describe the influence of cavity distortion in refractometry.

[6] Equation (5) shows that when the mirror penetration depth and the Gouy phase are neglected, it is adequate, as was done in some works in which specific features of the technique were scrutinized, e.g. [35, 41, 42, 52], for the case when the gas pressure and the cavity deformation are restricted so that $(n-1)\varepsilon'$ is negligible with respect to unity, to express the refractivity as

$$n-1=\frac{\frac{\Delta\nu}{\nu_0}+\frac{\Delta m}{m_0}}{1-\frac{\Delta\nu}{\nu_0}+\varepsilon}, \quad (7)$$

where ε is defined as $\frac{\delta L}{L_0}\frac{1}{n-1}$.

[7] Although this is a recursive equation in $n-1$, the recursivity is, in general, very weak; the $(n-1)\varepsilon'$ term in the denominator, which is the part of the $n\varepsilon'$ that carries the recursivity, seldom contributes to the assessed refractivity by more than a few times 10^{-6} on a relative scale. This implies that it is sufficient to utilize, in a recursive manner, a first order estimate of $n-1$ with solely one to two significant digits for the $(n-1)\varepsilon'$ term to obtain a relevant value for $n-1$.

[8] This shows that the presence of mirror penetration depth and the Gouy phase can be seen as a shift of the empty cavity laser frequency (transforming ν_0 to ν_0') and that the Gouy phase additionally provides a contribution that adds to the cavity deformation (transforming ε to $\frac{\Theta_G}{\pi m_0}+\varepsilon_0'$). It also shows that the quantum number q, which, as is shown in Eq. (4) in footnote 4, commonly

As is shown in Silander et al. [51] as well as in Appendix A, when the mirrors are not used around their center frequency, the cavity mode frequencies and refractivity given above, i.e. the Eqs. (2), (3), and (7) - (9), can be used as long as the $L_{\tau,c}$ and γ_c are replaced by $L_{\tau,s}$ and γ'_s, which are given in terms of $\tau_s(n)$, the GD at the center frequency of the light, and $\Delta\nu_{cs}$, the frequency difference between the mirror center frequency and the center of the working range, given by $\nu_c - \nu_s$.

3.1.2 Dual-FP-cavity refractometry

As was alluded to above, for improved performance, refractometry is often implemented in DFPC systems. This implies that the change in refractivity, in practice, is assessed as a shift in the beat frequency between the frequencies of two lasers, one addressing the measurement cavity, and one probing the reference cavity, when gas is let into (or evacuated from) the former one [41, 47, 52, 53, 55].

In this case, each laser is locked to its own cavity. The shift in the frequency of the measurement cavity is then assessed as a shift in the beat frequency between the two laser frequencies, f, given by $\mid \nu_r - \nu_m \mid$, where ν_r and ν_m are the frequencies of the measurement and reference lasers (addressing the measurement and reference cavities), respectively. This implies that Eq. (9), instead of being expressed in terms of the shift of the frequency of the measurement cavity, $\Delta\nu$, can alternatively be expressed in terms of the shift of the beat frequency, Δf, which is given by the difference in the beat frequencies when measurement cavity is empty and filled with gas, respectively, i.e. as $f^{(0)} - f^{(g)}$, and, in case any possible change in the number of the mode addressed in the reference cavity take place, additionally also in this.

3.1.3 Procedures and expressions for the GAMOR methodology

Although the expressions above provide adequate estimates of the refractivity in the ideal case, since the evacuated and the filled measurement cavity beat frequencies [i.e. the $f^{(0)}$ and the $f^{(g)}$, respectively] cannot be assessed simultaneously, the assessed refractivity will be affected by the presence of various types of disturbances that the system can be exposed to, predominantly fluctuations [43] and drifts [44]. To mitigate the effect of such types of disturbances, the GAMOR methodology incorporates a process in which the evacuated measurement cavity beat frequency, $f^{(0)}$, is, for each gas modulation cycle, not assessed at a single instant; it is instead estimated for all time instants of the modulation cycle by the use of a linear interpolation between two evacuated measurement cavity beat frequency assessments performed in rapid succession — one performed directly prior to the gas filling of the measurement cavity and another directly after it has been evacuated. By this, the evacuated measurement cavity beat frequency can be estimated at all times during a modulation cycle, including those when the measurement cavity contains gas without any need to specifically assess any amount of disturbance (drifts of fluctuations).

However, it should be noticed that although this interpolation procedure is straightforward when there are no mode hops in the reference cavity and when the measurement laser, for every modulation cycle, originates from, and return to, the same mode, above assumed to be the m_0 mode, this is not the case in general. Because of such mode jumps, the beat signal f is, in such cases, a non-continuous (i.e. a wrapped) function. In order to accommodate for also such situations, it has been found convenient to create an unwrapped (i.e. a mode-jump-corrected) beat frequency, f_{UW}, defined as

$$f_{UW} = \pm f - \left(\frac{\Delta m_m}{m_{0m}} \nu'_{0m} - \frac{\Delta m_r}{m_{0r}} \nu'_{0r} \right), \qquad (10)$$

where Δm_m and Δm_r are the numbers of mode jumps the measurement and reference lasers have made from the modes m_{0m} and m_{0r} at which their empty cavity frequencies, ν'_{0m} and ν'_{0r}, were assessed.[9] The $\pm$ sign refers to the cases when $\nu'_{0m} > \nu'_{0r}$ and $\nu'_{0m} < \nu'_{0r}$, respectively [47, 52].

The unwrapped empty measurement cavity beat frequency, $f^{(0)}_{UW}$, which represents the beat frequency

is used when the mirror penetration depth and the Gouy phase are neglected, is related to m, which, according to Eq. (1), is the relevant mode number in the presence of the aforementioned concepts, by $q = m + \frac{\Theta_G}{\pi} + n\gamma_c$.

[9] ν'_{0m} and ν'_{0r} are given by $\nu_{0m}/(1+\frac{\Theta_G}{\pi m_{0m}}+\frac{\gamma_c}{m_{0m}})$ and $\nu_{0r}/(1+\frac{\Theta_G}{\pi m_{0r}}+\frac{\gamma_c}{m_{0r}})$, respectively, where, in turn, ν_{0m} and ν_{0r} are the measured empty cavity frequencies of the measurement and reference cavities, respectively. Moreover, Δm_r accounts for a possible shift in the mode addressed in the reference cavity when gas is let into the measurement cavity. For a well-designed, stable system, this entity is often zero.

the system would have provided if both lasers would have been at the modes at which the empty cavity frequencies were assessed, i.e. at m_{0m} and m_{0r}, has thus the property that it is continuous even if any of the lasers make any mode hop, and is thereby suitable for the interpolation process.

This implies that the interpolation, for modulation cycle k, can be estimated, for all times that fulfills $t_k < t < t_{k+1}$, as

$$\tilde{f}^{(0)}_{UW}(t_k,t,t_{k+1}) = f^{(0)}_{UW}(t_k) + \frac{f^{(0)}_{UW}(t_{k+1}) - f^{(0)}_{UW}(t_k)}{t_{k+1}-t_k}(t-t_k). \quad (11)$$

This process is schematically illustrated by the green straight line in panel c in Fig. 3 shown in section 4.2 below.

This implies, in turn, that at each instant during which the filled measurement cavity assessment is evaluated during modulation cycle k (which predominantly takes place during the last part of the filled measurement cavity section of the gas modulation cycle) the shift in beat frequency between the two laser fields most suitably can be assessed as

$$\Delta f_{UW}(t) = f^{(g)}_{UW}(t) - \tilde{f}^{(0)}_{UW}(t_k,t,t_{k+1}). \quad (12)$$

This is schematically shown by the curve in panel d in Fig. 3 below.

As has been shown by Silander et al. [52], based on these expressions, the refractivity, $n-1$, can then, when nitrogen is addressed,[10] be straightforwardly and expediently expressed as a function of the shift of the unwrapped beat frequency, Δf_{UW}. In this case, Eq. (9) can be written as

$$n-1 = \frac{\frac{|\Delta f_{UW}|}{\nu'_{0m}}}{1 - \frac{|\Delta f_{UW}|}{\nu'_{0m}} + \frac{\Delta m_m}{m_{0m}} + \frac{\Theta_G}{\pi m_0} + \varepsilon'_0}. \quad (13)$$

The refractivity, $n-1$, is then finally assessed as the average of $(n-1)(t)$, calculated from Eq. (13) with $\Delta f_{UW}(t)$ given by Eq. (12), over a suitable time interval of the filling measurement cavity section (for the case with 100 s long gas modulation cycles, typically for 10 s, between 40 and 50 s after the filling of the measurement cavity), schematically illustrated by the data points within the red circle in panel d in Fig. 3 below.

As is discussed in some detail below, by this the influence of several types of disturbances, comprising noise, fluctuations, and drifts, can be efficiently mitigated [41, 43, 44].

It could finally be concluded that Eq. (13) provides a convenient means to assess refractivity from a variety of systems using repeated fillings and emptyings of the measurement cavity, in particular those that assess pressure on a "real-time" basis, not only when the GAMOR methodology is utilized.

3.1.4 A note on the uncertainty in assessments of refractivity

When the major influence of fluctuations and drifts have been mitigated the uncertainty of the refractivity is given by the remaining uncertainty in both a number of assessed entities, predominantly Δf, ν_0, Δm_m and m_{0m}, and some system parameters, mainly A_R, Θ_G, γ_c (or γ'_s), and ε' (or ε'_0), together with some virial coefficients (see below as well as Ref. [50]).

It should be noticed that, for all pressures except the lowest ones (i.e. from a few kPa and above), the leading term in the expression for the refractivity in Eq. (13) is the $\frac{\Delta m_m}{m_{0m}}$ part of the $\frac{|\Delta f_{UW}|}{\nu'_{0m}}$ entity [denoted $\frac{\Delta m}{m_0}$ in Eq. (5)].

It should be clear that Δm_m (and Δm) can be assessed without any uncertainty (since they are in general one- or two-digit integers). It should additionally be noticed that, since m_{0m} (and m_0) represent mode numbers, they are also integers. As can be deduced from Eq. (2), the latter ones can most conveniently be assessed as the closest integer to the ratio of ν'_0 and the free-spectral-range (FSR), i.e. as $Int\left(\frac{\nu'_0}{FSR}\right)$, where the FSR is defined as $\nu(m_0+1)-\nu(m_0)$ and given by $\frac{c}{2L'_0}$. This implies that, as long as ν'_0 and FSR have sufficiently small relative uncertainties (typically both $< \frac{1}{2m_{0m}}$), also m_{0m} can be assessed without any uncertainty. This implies that the leading term in the numerator in the expression for the refractivity, i.e. the $\frac{\Delta m_m}{m_{0m}}$ part of the $\frac{|\Delta f_{UW}|}{\nu'_{0m}}$ entity (or the $\frac{\Delta m}{m_0}$), in practice does not provide any uncertainty. This implies that, for the case when $\Delta f \approx 0$, the main uncertainty in the assessment of refractivity lies in the uncertainty of ε'_0.

A procedure for how to assess ε'_0 with an accu-

[10] For the case when any other gas is addressed, Eq. (13) should be exchanged to a correspondingly one based on Eq. (5).

racy contributing in the low parts-per-million (ppm, 10^{-6}) range has recently been developed by Zakrisson et al. [50]. This procedure is further described in section 7.3.3 below. A description of how the concept of pressure-induced deformation has been addressed in the "QuantumPascal" project is given in a separate guide [60].

3.2 Molar Density

For pressures up to atmospheric ones, of most gases, including nitrogen, the molar density can be calculated by assessing the refractivity and using the extended Lorentz–Lorenz equation as

$$\rho = \frac{2}{3A_R}(n-1)[1 + b_{n-1}(n-1)], \qquad (14)$$

where b_{n-1} is given by $-(1 + 4B_R/A_R^2)/6$, where, in turn, B_R is the second refractivity virial coefficient in the Lorentz–Lorenz equation [10, 35, 42].

3.3 Pressure

The molar density can then be used to assess, by use of an equation of state, the pressure, e.g. as

$$P = RT\rho[1 + B_\rho(T)\rho], \qquad (15)$$

where $B_\rho(T)$ is the second density virial coefficient.

For more detailed descriptions of the Lorentz–Lorenz equation and the equation of state, and, for expressions valid for higher pressures (when higher order virial coefficients need to be included), the reader is referred to the literature, e.g. [9–12, 17, 35, 42, 61].

3.4 Molecular Data

The most frequently addressed gas has so far been nitrogen. Table 1 provides information about the relevant gas constants for nitrogen, A_R, b_{n-1}, and B_ρ, at 302.91 K and 1550.14 nm, which represent the conditions under which the most accurate assessments with the Invar-based DFPC refractometry system utilizing the GAMOR methodology described below have been performed (see below) [50].

Table 1. Gas coefficients for N_2 at 302.91 K and 1550.14 nm.

Coef.	Value (k = 2)	Reference
A_R	4.396549(34) × 10^{-6} m^3/mol	[50, 61]
b_{n-1}	−0.195(7)	[30, 50]
B_ρ	−4.00(24) × 10^{-6} m^3/mol	[50, 61]

4 Theoretical analysis and explication of the ability of the GAMOR methodology to automatically mitigate the influence of disturbances

As was alluded to above, independent of whether the GAMOR methodology is used or not, all assessments of refractivity (and thereby pressure) by refractometry must rely on (at least) two assessments, one with and one without gas in the measurement cavity. It has been found that the two cornerstones of the GAMOR methodology, viz. a short time separation between these two assessments and, to assess the empty measurement cavity beat frequency at the time when the filled measurement cavity assessment is performed, the use of interpolation between two evacuated measurement cavity beat frequency assessments, one performed before and one after the filled cavity assessments, play an important role in the extent to which the assessment of refractivity is influenced by various types of disturbances the system is exposed to.

To properly assess the ability of the GAMOR methodology to reduce the influence of various types of disturbances on the assessment of refractivity, two scientific works dedicated to the concept have been published; one, regarding the ability of gas modulation to mitigate the influence of fluctuations in refractometry, was performed just prior to the initiation of the EMPIR QuantumPascal project [43], while the other, addressing the ability of the GAMOR methodology to mitigate the influence of drifts [44], was made as a part of the project.[11]

[11] The reason for treating fluctuations separately from drifts was that the two types of disturbances, which appear at dissimilar time scales, affect refractometry assessments dissimilarly and they therefore need to be described in different manners (mathematically modelled as Fourier and Taylor series, respectively).

4.1 Ability of the GAMOR methodology to mitigate the influence of fluctuations

The first cornerstone of GAMOR advocates the use of a frequent referencing of filled measurement cavity beat frequencies to evacuated cavity beat frequencies, which is synonymous to using short gas modulation cycles. To provide an intuitive understanding of how the length of the gas modulation cycle[12] can influence how much of a given fluctuation the detection process will pick up (or be affected by), a theoretical description was developed for the influence of fluctuations, modeled as a set of Fourier components, on refractometry in the absence and presence of gas modulation [43].

Figure (1) displays, by the panels (a) and (c), a schematic illustration of the gas filling-and-emptying process for DFPC refractometry when assessing a pressure of 2 kPa in the absence and presence of gas modulation, respectively. The panels (b) and (d) show the developments of the associated beat frequencies in the presence of an individual Fourier component of a fluctuation, f_D. For illustrative purposes, it was assumed that the period of the Fourier component is similar to the gas modulation period in the unmodulated case. Since the latter most often is significantly longer than the modulation period when gas modulation is utilized, the period of the fluctuation will be significantly longer than the modulation period of the modulated assessments.[13]

The instants for the two beat frequency measurements in the panels (a) and (b) are marked by vertical dashed lines (the left and right lines represent the time instants for the empty and the filled measurement cavity assessments, respectively). Although there is one pair of beat frequency assessments for each modulation cycle when gas modulation is utilized, again for illustrative purposes, vertical lines

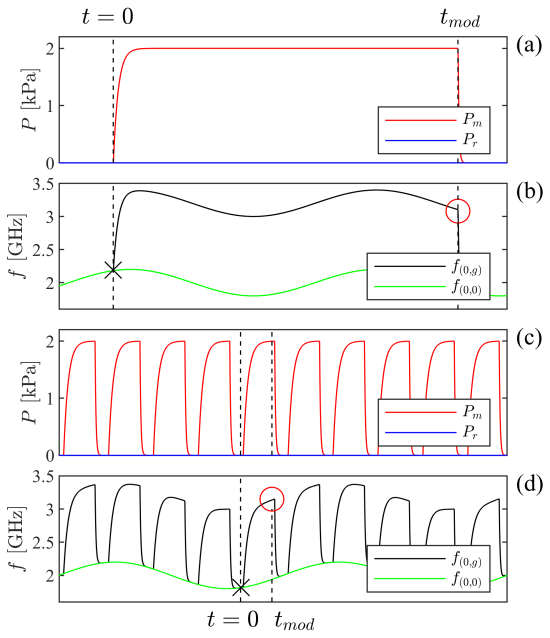

Figure 1. Schematic illustration of the gas filling-and-emptying process and the measured beat frequencies when a pressure of 2 kPa is assessed in the presence of a single Fourier component of fluctuations for unmodulated [the panels (a) and (b)] and modulated [the panels (c) and (d)] refractometry. The panels (a) and (c) represent the pressures of the two cavities [the upper (red) curves, those of the measurement cavity; the lower (blue) curves, those of the reference cavity]. The panels (b) and (d) indicate the corresponding beat frequencies [the upper (black) curves, the actual beat frequency when the measurement cavity is filled with gas, i.e. $f^{(g)}(t)$, in the figure denoted $f_{(0,g)}(t)$; the lower (green) curves, the empty measurement cavity beat frequency, $f^{(0)}(t)$, denoted $f_{(0,0)}(t)$]. Note that, for display reasons, the gas modulation period for the modulated case is only one-tenth of that of the unmodulated case, although, in reality, it is significantly shorter (typically 3 orders of magnitude shorter). Reproduced with permission from Ref. [43].

have been associated to only one cycle in the panels (c) and (d). Each assessment of beat frequency,

[12] When unmodulated refractometry is performed, it is natural to see the time separation between the empty and filled measurement cavity assessments as "the gas exchange time", while, when gas modulation is utilized, the same entity alternatively is referred to as the "length of the gas modulation cycle", or simply the "gas modulation period". To be able to compare various modes of operation of refractometry (primarily unmodulated and modulated refractometry), we will henceforth denote all these either the "length of the gas modulation cycle" or the "gas modulation period" and denoted them t_{mod}.

[13] Note though that although Fig. (1) depicts the modulated case with a gas modulation period that is solely one order of magnitude shorter than what it is in the unmodulated case, in reality the relative difference between the two cases is significantly larger: often they differ by three orders of magnitude or more.

marked, for the illustrated cycle, by a circle and a cross for when the measurement cavity is filled with gas and emptied, respectively, comprises an averaging over several data points for a time that is significantly shorter than the length of the gas modulation cycle in the modulated case, typically 10 s.

The model developed and presented in Ref. [43] was then used to estimate the fractions of specific Fourier components of a given fluctuation the system picks up as a function of its (Fourier) frequency for two different lengths of the gas modulation cycle (t_{mod}), 10^5 s (corresponding to 28 hours) and 10^2 s, representing typical unmodulated and modulated conditions, respectively. As is shown in that work, it was found that a given refractometry system indeed picks up dissimilar amounts of fluctuations depending on the modulation condition.

Figure (2) displays, by the coloured curves in the panels (a) and (b), the fraction of specific components of fluctuations the system picks up as a function of their Fourier frequency for the case of unmodulated detection (with a gas filling period of 10^5 s) and with gas-modulated detection (with a modulation period of 10^2 s), respectively. To guide the eye, the black straight lines represent the envelopes of the structured responses.

As can be seen from the leftmost parts of the two panels, the system will pick up only minor fractions (below unity in the figure) of the fluctuations whose Fourier frequencies are lower (smaller) than the inverse of the length of the gas filling/modulation cycle [i.e. $< 1/(2\pi t_{mod})$]; as indicated by the slanted lines in the graphs, for such modulation cycles, it will only pick up a fraction $2\pi f_D t_{mod}$ of the fluctuation. Since t_{mod} is much shorter when the system is modulated than when it is not, this implies that when a refractometry system is run under modulated conditions, it will pick up significantly less of any such fluctuations than when it is run unmodulated.[14] This

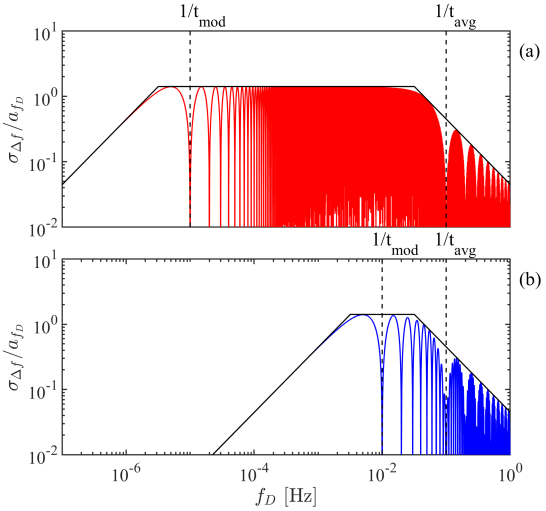

Figure 2. The fraction of specific components of fluctuations the system picks up as a function of its Fourier frequency, f_D, for two different lengths of the gas modulation cycle (t_{mod}), representing, in panel (a), unmodulated detection with a gas modulation period of 10^5 s, and, in panel (b), with gas-modulated detection, utilizing a modulation period of 10^2 s. In both cases, an averaging time (t_{avg}) of 10 s has been assumed. The colored curves represent the response averaged over all possible phases between the fluctuations and the detection. The black lines are the envelopes of the responses. Reproduced with permission from Ref. [43].

shows that, irrespective of other properties of the system, a refractometry system will always pick up less amount of fluctuations when it is run modulated than when it is run unmodulated.[15]

Hence, in agreement with what has been concluded about other types of modulation techniques in metrology, e.g. frequency and wavelength mod-

[14] For the specific case considered in Fig. (2), when being unmodulated (the uppermost panel), it will primarily be affected by (and thus pick-up) fluctuations with Fourier frequencies above $(1/2\pi)10^{-5}$ Hz (corresponding to fluctuations whose periods are shorter than $2\pi 10^5$ s) while, when being modulated (the lowermost panel), it will primarily solely be affected by fluctuations whose frequencies are above $(1/2\pi)10^{-2}$ Hz (corresponding to fluctuations with periods shorter than $2\pi 10^2$ s). The influence of fluctuations with Fourier frequencies below $(1/2\pi)10^{-2}$ Hz (corresponding to fluctuations whose periods are longer than $2\pi 10^2$ s) will thus be mitigated significantly more when the system is run with modulation than when it is not. For Fourier frequencies below $(1/2\pi)10^{-5}$ Hz, this is given by the ratio of the lengths of the gas modulation cycles in the two cases, in this particular case by three orders of magnitude.

[15] The figure also shows that the modulation procedure reduces the influence of fluctuations with other frequency components than what the conventionally used averaging processes mitigate (which decrease the influence of fast fluctuations, i.e. the components whose Fourier frequencies are higher than the inverse of the integration time, i.e. the frequencies that are $> 1/(2\pi t_{avg})$ [corresponding to fluctuation components whose period is $< (2\pi t_{avg})$]; as is shown by the rightmost parts of the panels, in this case, the components whose period is $< 2\pi 10$ s.

ulation spectrometry [62–65], the model indicates that rapid gas modulation has the ability to reduce the influence of a significant fraction of the low-frequency fluctuations [primarily those whose frequency is below $< 1/(2\pi t_{mod})$] that often are the dominating ones in measurement systems (due to their anticipated $1/f$ dependence).[16]

4.2 Ability of the GAMOR methodology to mitigate the influence of drifts

The two cornerstones upon which the GAMOR methodology relies (modulation and interpolation) also contribute to a mitigation of the influence of drifts. However, it has been found that they do not do so to the same extent for all types of drifts. Reference [44] therefore provides a comparison (both an estimate based on a theoretical analysis and an experimental assessment) of the extent to which several types of refractometry methodology[17] are affected by various types of drifts.[18]

4.2.1 Qualitative description

To depict the ability of the GAMOR methodology to mitigate the influence of campaign-persistent (i.e. type I) drifts, and to illustrate the roles the two cornerstones have in this process, the response of a system exposed to this type of drift probed by the GAMOR methodology (for simplicity, in the absence of mode jumps) is schematically depicted in Fig. (3).

Panel (a) illustrates the pressure in the measurement cavity (upper red curve), which is alternately evacuated and filled with gas while the reference cavity (lower blue curve) is held at a constant pressure (in this case for simplicity chosen to be at vacuum). For the case with a drift of type I, the frequencies of both the measurement and the reference lasers, shown in panel (b), will be affected (although possibly to dissimilar extent). This implies that the beat frequency, assessed as the difference between the two curves in panel (b), displayed by the uppermost (black) curve in panel (c),[19] likewise will be affected by the drifts.

The lower green line in the same panel, which has been constructed according to Eq. (11) as a linear interpolation between two evacuated measurement cavity assessments, indicated by × markers, represents the estimated inter-cycle interpolated evacuated measurement cavity beat frequency.[20]

Panel (d), finally, displays, by the sole black curve, the drift-corrected shift in beat frequency, $\Delta f(t)$, given by the difference between the two curves displayed in panel (c), i.e. the difference between the beat frequency measured when the measurement cavity contains gas and the interpolated evacuated measurement cavity beat frequency, $f^{(g)}(t) - \tilde{f}^{(0)}_{UW}(t)$. The value of the drift-corrected shift in beat frequency at the position of the red circle, $\Delta f(t_g)$, represents the data used for the assessments of refractivity by use of Eq. (13) above.

This schematic illustration thus indicates graphically, and thereby qualitatively, that the influence of drifts can efficiently be mitigated by the interpo-

[16] It is worth to note that the analysis above, as well as Ref. [43], refer to the influence of solely one of the two cornerstones of the GAMOR methodology on the assessment of refractivity, viz. (i). However, cornerstone (ii) will additionally mitigate the influence of fluctuations when the GAMOR methodology is utilized. The influence of cornerstone (ii) on the ability to mitigate the influence of disturbances is analyzed in some detail below though when the ability to mitigate the influence of drifts is scrutinized.

[17] The methodologies considered are: Unmodulated noninterpolated (UMNI) refractometry [both single-FPC (SFPC) refractometry and DFPC refractometry]; unmodulated interpolated (UMI) refractometry; modulated noninterpolated (MNI) refractometry; and GAMOR, representing modulated interpolated refractometry.

[18] It was found suitable to distinguish between the drifts that affect the cavity mode frequencies persistently and continuously during the entire measurement campaign, irrespective of the state of the gas modulation cycle, referred to as campaign-persistent drifts (type I), from those that are reset once per gas modulation cycle by the gas modulation process (so the drift process starts over for each modulation cycle), referred to as cycle-limited drifts (type II). The type II drifts, in turn, are separated into two subcategories, viz., those that affect the refractivity of the gas in the reference and measurement cavities, (a) and (b) respectively. Drifts of the physical lengths of the cavities are thus of type I. Leakages and outgassing into the reference cavity represent drifts of type I if the reference cavity is sealed off during the entire measurement campaign while they constitute drifts of type IIa if the reference cavity is evacuated once per gas modulation cycle. Leakages or outgassing into the measurement cavity are of type IIb.

[19] The derivation and analysis made in Ref. [44] were made under the condition that the drift does not induce any mode hop. The scrutiny was therefore based on the measured beat frequency f instead of the unwrapped beat frequency f_{UW} (which include such) on which the theoretical description given in this work relies. To adhere to the plots and graphs presented in that work, and since it will not affect the conclusions, we have, in this section, retained the notation f for the beat frequency.

[20] The red and the green circles in panel (c) represent the values of the beat frequency at the time when the filled measurement cavity assessment is performed, $f^{(g)}(t_g)$, and the evacuated measurement cavity beat frequency, estimated by interpolation, at the same time, $\tilde{f}^{(0)}(t_g)$, in the figure denoted $f(t_g)$ and $\tilde{f}_{(0,0)}(t_g)$, respectively.

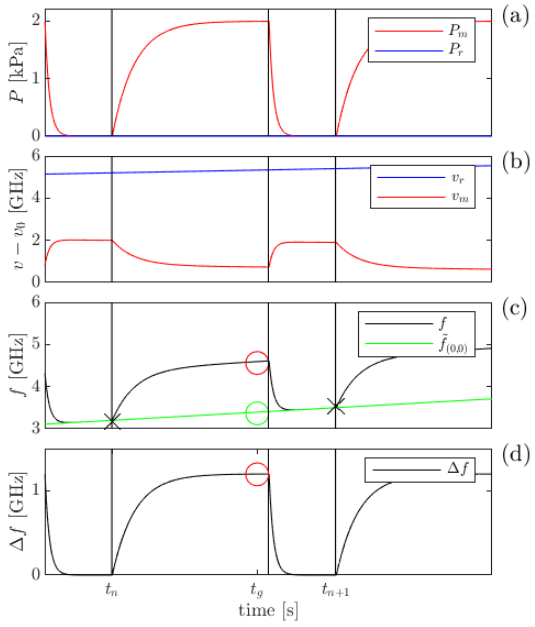

Figure 3. **The principles of GAMOR on a system exposed to drifts of type I displayed over two modulation cycles. Panel (a) displays, by the upper red and the lower blue curves, the pressures in the measurement and reference cavities, respectively, as functions of time. Panel (b) shows the corresponding frequencies of the two lasers (for display purposes, in the absence of mode jumps and offset to a common frequency). Panel (c) illustrates, by the upper black curve, the corresponding beat frequency. The × markers represent empty cavity beat frequency assessments while the green line, denoted $\tilde{f}_{(0,0)}(t)$, corresponds to the inter-cycle evacuated measurement cavity beat frequency, in Eq. (11) denoted $\tilde{f}^{(0)}_{UW}(t)$, constructed as a linear interpolation between the two evacuated measurement cavity assessments. Panel (d) displays the drift-corrected shift in beat frequency, denoted Δf, corresponding to $\Delta f_{UW}(t)$ in Eq. (13), given by the difference between the beat frequency measured with gas in the measurement cavity, $f^{(g)}_{UW}(t)$, and the "baseline", given by the interpolated evacuated measurement cavity beat frequency, $\tilde{f}^{(0)}_{UW}(t)$. Reproduced with permission from Ref. [44].**

lation procedure that constitutes one of the cornerstones of GAMOR.

4.2.2 Quantitative analysis

To quantitatively assess the ability of GAMOR to reduce the influence of campaign-persistent drifts, such a drift of the evacuated measurement cavity beat frequency, modelled with both linear and nonlinear contributions according to the Eqs. (B.1)-(B.3) in Appendix B (and further defined there), is illustrated by the uppermost curve in the center of the graph in Fig. (4).

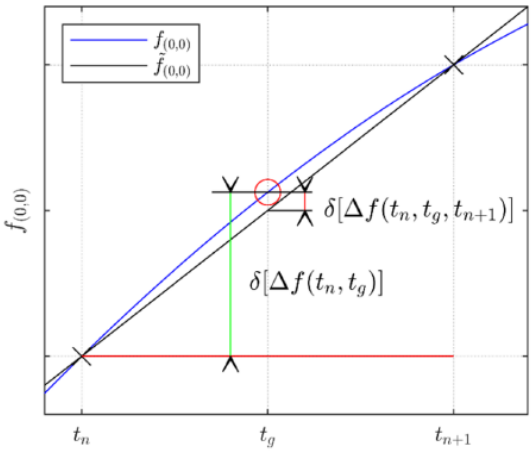

Figure 4. **Blue solid curve (the uppermost in the center of the graph): the evacuated measurement cavity beat frequency, $f^{(0)}(t)$ [in the figure denoted $f_{(0,0)}(t)$], for modulated refractometry in the presence of drifts. The beat frequency at time at which the gas measurement is performed is marked by a red circle. The beat frequencies measured at the times of an empty measurement cavity are marked by crosses (×). Reproduced with permission from Ref. [44]**

Since, in the unmodulated case, the shift of the beat frequency used for assessment of refractivity by the Eqs. (10) - (13) is given by the difference between the beat frequency measured when there is gas in the measurement cavity at the time instant t_g and that when it is evacuated at t_n, the error in the assessment of the beat frequency is given by the shift in the evacuated measurement cavity beat frequency between these two time instants, $f^{(0)}(t_g) - f^{(0)}(t_n)$,

referred to as $\delta[\Delta f(t_n, t_g)]$. This entity is represented by the long (leftmost) green vertical line in Fig. (4).

For the interpolated methods, such as GAMOR, the evacuated measurement cavity beat frequency is given by an estimated inter-cycle interpolated evacuated measurement cavity beat frequency, $\tilde{f}^{(0)}(t)$, calculated based on two evacuated cavity measurement beat frequencies [in Fig. (4) denoted $f^{(0)}(t_k)$ and $f^{(0)}(t_{k+1})$, and represented by the crosses]. This interpolation, which is based on Eq. (11) and corresponds to the straight green line in Fig. (3c) above, is given by the straight slanted line in Fig. (4). The figure shows that the error made when an interpolated methodology (e.g. GAMOR) is used, which is given by the difference between the real and the interpolated evacuated cavity measurement beat frequencies, denoted $\delta[\Delta f(t_n, t_g, t_{n+1})]$, is given by $f^{(0)}(t_g) - \tilde{f}^{(0)}(t_g)$, represented by the short (rightmost) red vertical line.

As can be deduced from Fig. (4) together with the Eqs (B.1) - (B.3) in Appendix B, and as is further discussed in Ref. [44], this implies that while non-interpolated refractometry is mainly affected by the linear parts of the drift, given by

$$\delta[\Delta f(t_n, t_g)] = \left(\frac{\partial f^{(0)}}{\partial t}\right)_{t_g} t_{mod}, \qquad (16)$$

the corresponding entity in the case with interpolation is predominantly affected solely by the first non-linear contribution to the drift, i.e.

$$\delta[\Delta f(t_n, t_g, t_{n+1})] = -\frac{1}{2}\left(\frac{\partial^2 f^{(0)}}{\partial t^2}\right)_{t_g} t_{mod}^2, \qquad (17)$$

where the $(\partial f^{(0)}/\partial t)_{t_g}$ and $(\partial^2 f^{(0)}/\partial^2 t)_{t_g}$ represent the amount of linear and first order non-linear drift of empty cavity mode frequency, respectively.

This clearly illustrates the important fact that while non-interpolated methodologies are affected by the linear part of the drifts, i.e. by the $(\partial \nu_i^{(0)}/\partial t)_{t_g}$ entity, when interpolation is used, it is solely influenced by non-linear parts of the drift, predominately by the $(\partial^2 \nu_i^{(0)}/\partial^2 t)_{t_g}$ entity. This implies that when interpolation is used, the assessment is not influenced by the dominating linear parts of the drift. Neither is it necessary to separately assess the linear parts of the drifts (as must be done when drifts are explicitly corrected for when non-interpolated methodologies are used); its influence is automatically mitigated by the interpolation procedure.

The Eqs. (16) and (17) also show that, in both cases, the amount of drift the measurements are influenced by depends on the length of the modulation period — the shorter the modulation period, the lesser the technique will be affected by drifts, and more so for an interpolated methodology than for a non-interpolated one.

All this illustrates the ability of the GAMOR methodology, which encompasses both short gas modulation periods and an interpolation process, to reduce the influence of drift (in this case of type I), and to do this in an automated manner.

The interested reader is referred to Ref. [44] for a further description of its ability to reduce the influence of other types of drift.

5 Experimental Setup

5.1 GAMOR instrumentation - General realization

A GAMOR instrumentation comprises basically two main parts, a refractometry system and a gas handling system.

The refractometry systems so far realized for GAMOR have all been utilizing a DFPC [41–58]. In addition to the cavity system, they contain a number of optical, acousto-optic, and electro-optic devices used to control, modulate, and assess the frequency of the light.

The gas handling system connects the cavities with a gas supply, the device whose pressure is assessed, and a gas evacuation system. It contains a number of valves and tubing that control the filling and evacuation of the cavities in a predetermined manner in such a way the system is fully autonomous; it can work unattended 24/7 for any length of time.

Over the years, several "generations" of instrumentation have been developed. Since Invar is a material that has a number of advantageous properties for refractometry (see section 7.2.3 below), and since the GAMOR methodology can automatically mitigate the drawbacks of its unfavourable properties, after some initial proof-of-concept demonstrations using a cavity spacer of Zerodur [36, 41, 42], the most recent refractometry system has been con-

structed around an Invar-based DFPC system. This system, which has shown best performance and therefore has been used the most lately, is shortly described below and henceforth referred to as the "Invar-based DFPC system". A more detailed description is given elsewhere [45–47, 52].

5.2 The Invar-based DFPC system

5.2.1 The refractometry system

The Invar-based DFPC system, shown in Fig. 5, comprises an Invar-based DFPC that is precision machined from a ∅60 mm Invar rod [45]. The outer dimensions of the spacer are 160×60×50 mm. Each cavity consists of two ∅12.7 mm highly reflective (99.997%) plano-concave mirrors. Each mirror is placed in 6 mm deep clearance hole in the 160 mm long spacer and clamped by a back plate onto the ∅6 mm bores. This yields a mirror separation of 148 mm. This reflectivity and mirror separation result in a finesse of 10^4 and, for the wavelength used, an FSR of 1 GHz.

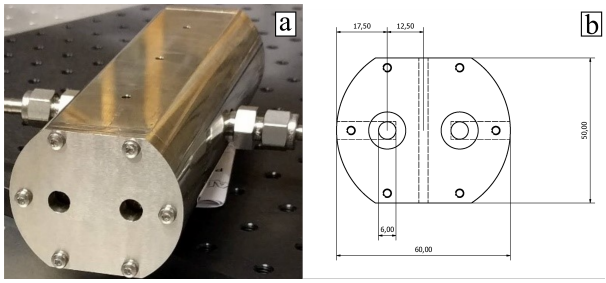

Figure 5. Panel (a): The Invar cavity assembly before being equipped with temperature probes and mounted inside the aluminium oven. The plates screwed into the spacer at its short ends press the mirrors, via O-rings, onto the spacer. Panel (b): A schematic drawing of the cavity assembly. Units in mm. Reproduced with permission from Ref. [48].

The refractometer system comprises a number of devices that make possible an efficient and expeditious probing of longitudinal cavity modes of the DFPC. A schematic of the system is shown in Fig 6.

Each cavity is probed by the light from an Er-doped fiber laser at a wavelength of 1.55 µm. Since this wavelength is in the data communication NIR region, there are plenty of fiber-connected devices

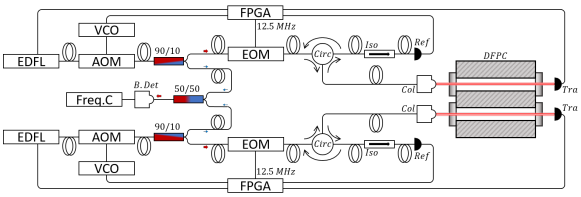

Figure 6. Schematic illustration of the refractometer setup. EDFL: Er-doped fiber laser; AOM: acousto-optic modulator; 90/10: 90/10 fiber splitter; EOM: electro-optic modulator; Circ: optical circulator; Iso: optical isolator; Ref: fast photodetector for the reflected light; Col: collimator; DFPC: dual-Fabry-Perot cavity; Tra: large area photodetector for the transmitted light; FPGA: field programmable gate array, VCO: voltage controlled oscillator; 50/50: 50/50 fiber coupler; B. Det: fast fiber-coupled photodetector for the beat signal; and Freq. C: frequency counter. Reproduced with permission from Ref. [48].

available. This does not only facilitate the realization of the system, it is also the basis for the sturdiness and reliability of the system.

The light is coupled into a fiber-coupled acousto-optic modulator (AOM) that uses the acousto-optic effect to shift (by diffraction) the frequency of light using a sound wave. Its first order output, which contains the frequency up-shifted component of the laser light, is coupled to a 90/10 fiber splitter.

The 90% output from the splitter is coupled into an electro-optic modulator (EOM) that, by phase modulation, produces sidebands (at 12.5 MHz) on the monochromatic laser beam for the locking of the laser light to a cavity mode by the Pound-Drever-Hall (PDH) locking technique [66].

The output of the EOM is coupled to an optical circulator (Circ) whose first order output is fed to a custom built collimator (Col). The output of the collimator, which is mode matched to a TEM_{00} mode of the cavity, is sent to the cavity. The reflected light, which carries information for the PDH locking, is coupled back into the collimator and routed via the second output of the circulator and an optical isolator (Iso) to a fast photodetector (Ref). The light transmitted through the cavity is monitored by a large area photodetector (Tra).

Each reflection detector is connected to a field programmable gate array (FPGA) that demodulates

the signal at the modulation frequency (12.5 MHz) to produce the PDH-error signal. Its slow components (<100 Hz) are sent to the EDFL-piezo, which provides the "slow" tuning of the frequency of the light, while the fast components (>100 Hz) are sent to a voltage controlled oscillator (VCO) that produces an RF-signal that drives the AOM around 110 MHz to correct for the rapid fluctuations.

To sample the beat frequency between the two cavities, the 10% outputs from the splitter in each arm are combined in a 50/50 fiber coupler (50/50). The combined light is routed to a fast fiber-coupled photodetector (B. Det) whose RF-signal is measured by a frequency counter (Freq. C). To account for mode jumps done by the automatic relocking routine, as is further discussed below, the voltages sent to the EDFL by the FPGA is monitored by an analogue input module (not in figure).

The refractometry system is described in more detail in [45].

5.2.2 The gas handling system

A schematic view of the gas handling system is given by Fig. 7. It consists of a combined inlet and gas regulating system, a combined valve control and cavity system, and a gas evacuation system.

The inlet system comprises a mass flow controller (MFC) connected to a gas supply, an electronic pressure controller (EPC), and a diaphragm filling valve (V_f) used together with the device that regulates the pressure (whose pressure is assessed), here, a dead weight piston gauge (DWPG). To reduce the risk for contamination of the gas in the volume prior to the filling valve, the output of the EPC is continuously evacuated by an oil-free rough pump resulting in a constant gas flow of gas from the MFC to the EPC.

The valve control system, which comprises four diaphragm valves connecting the two cavities to the gas filling and evacuation systems via separate paths (V_1, V_2, V_3, and V_4), is placed on top of the cavity system, where V_1 connects the gas system of the refractometer to the measurement cavity. All diaphragm valves are controlled by solenoid pilot valves (not in the figure) via a digital output module (not in the figure). The evacuation system comprises a molecular turbo pump backed by an oil-free rough pump.

To estimate the pressure under scrutiny, which is needed for assessment of mode jumps, a pressure gauge (High) is positioned between the filling valve and the cavity system valve control. To monitor the residual pressure, a low pressure gauge (Low) is positioned between the combined valve control and cavity system and the gas evacuation system.

The gas handling system is described in more detail in [47].

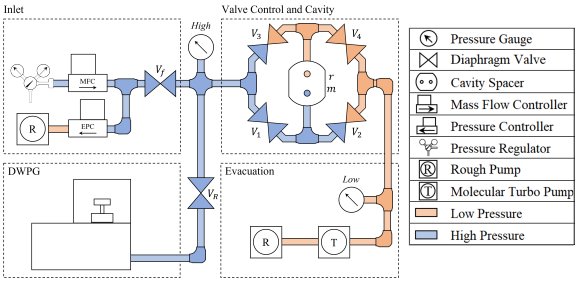

Figure 7. The gas handling system, comprising an inlet system, which, by sustaining a constant gas flow between the MFC and EPC reduces the risk for contamination of the gas in the volume prior to the filling valve (V_f), a combined valve control and cavity system, which connects the two cavities to the gas filling and evacuation systems (via valves V_1, V_2, V_3, and V_4), and a gas evacuation system, which evacuates the selected parts of the valve control and cavity system. MFC: mass flow controller; EPC: electronic pressure controller; T: turbo pump; R: oil-free rough pump; High: a high pressure gauge; Low: a low pressure gauge; and DWPG: dead weight piston gauge.

6 A cycle-resolved illustration of the operation and performance of the GAMOR methodology

As was stated above, the gas modulation process in GAMOR comprises a series of periodic modulation cycles of the pressure of gas in the measurement cavity while the pressure in the reference cavity is held constant (often constantly evacuated through valve 4).

To illustrate the data acquisition process, the role of the mode jumps, and the unwrapped beat frequency in the assessment of pressure, Fig. 8 shows some typical cycle resolved raw data from a 200 s long gas modulation cycle, distributed over a fill-

ing and an evacuation part of the cycle, each lasting 100 s (denoted t_I and t_{II}, defined in Fig. 9), for a pressure of 30.7 kPa [47]. The three panels in Fig. 8 display, for an individual modulation cycle, the measured beat frequency, $f(t)$, the cavity mode numbers, $\Delta m_i(t)$, for the two cavities, and the corresponding unwrapped beat frequency, $\Delta f_{UW}(t)$, as a function of time, respectively.

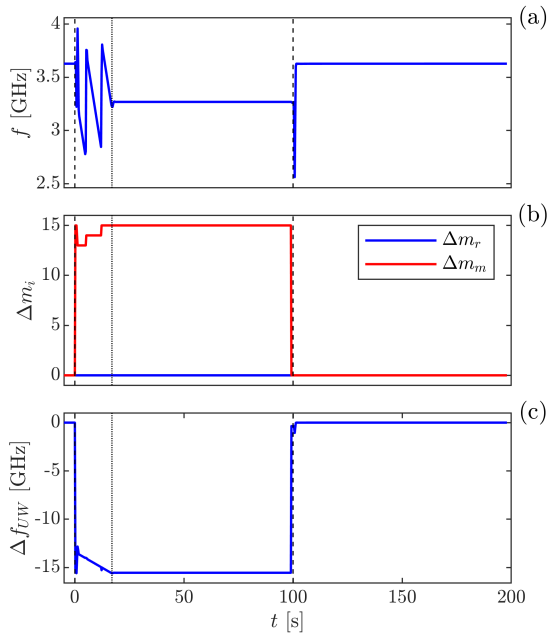

Figure 8. The time evolution of: panel (a); the measured beat frequency, $f(t)$; panel (b); the mode numbers addressed, $\Delta m_i(t)$ with i being either m or r representing the mode numbers addressed (with respect to m_{0i}) in the measurement and reference cavities, respectively; and panel (c); the corresponding unwrapped beat frequency, $\Delta f_{UW}(t)$, over a 200 s long modulation cycle assessing a pressure of 30.7 kPa. For a description of the various time intervals of the modulation cycle, see the figure caption of Fig. 9. Reproduced with permission from Ref. [47].

The modulation cycle is initiated (at time 0) by a closing of valve V_2 and, shortly thereafter, an opening of valve V_1, which, by volumetric expansion, results in an almost momentary increase of the pressure in the measurement cavity to around 85% of

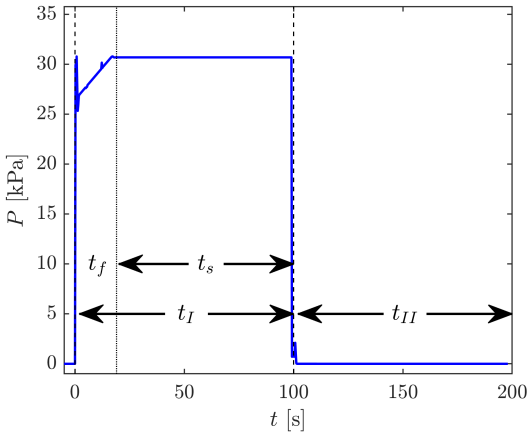

Figure 9. The time evolution of the assessed pressure during the 200 s long gas modulation cycle displayed in Fig. 8, $P(t)$. t_I represents the filling part and t_{II} the evacuation part of the gas modulation cycle, each being 100 s. t_f is the time during which the MFC is re-filling the system while t_s is the time during which the DWPG is stabilizing the pressure (i.e. when the piston is floating). Reproduced with permission from Ref. [47].

the set pressure. The MFC is then, for a time of 20 s (referred to as t_f in Fig. 9), until a so called set pressure is reached, filling up the system (by a constant increase of the pressure). As is shown by the panels (a) and (b) in Fig. 8, during this time, the frequency of the measurement laser changes rapidly; the beat frequency decreases as the pressure increases until the laser makes a mode jump, at which the beat frequency makes a sudden jump to a higher value. This process is repeated until the beat frequency is within the dynamic range of the frequency counter, which in this particular case is twice.

After the set pressure is reached (i.e. after ca. 20 s), the piston in the DWPG floats, which, for the remaining 80 s of the 100 s long filling part of the gas modulation cycle (denoted t_s in Fig. 9), results in a stabilization of the pressure at a constant pressure. As has been shown elsewhere, this provides sufficient time for the DWPG to produce a stabilized pressure and the DFPC to reach a thermal steady-state [48]. Data representing the filled measurement cavity assessment, $f_{UW}^{(g)}(t)$, is then taken during the last 10 s of the filling part of the gas modulation cycle

(i.e. between $t = 90$ and 100 s in the Figs. 8 and 9).

The measurement cavity is thereafter evacuated for 100 s. This takes place by closing valve V_1 and opening valve V_2, which results in a fast decrease in pressure, manifested by a sudden change in both the unwrapped beat frequency and the mode number addressed (a decrease in the latter). The empty measurement cavity beat frequency, $f_{UW}^{(0)}(t)$, is assessed during the last 10 s of this part of the modulation cycle.

When a full cycle is completed, the next one follows automatically.

The assessed signals in the panels (b) and (c) in Fig. 8, i.e. the Δf_{UW} and the Δm_i, are then converted into pressure by use of the Eqs. (12) - (15). Figure 9 shows the cycle resolved pressure, $P(t)$, calculated by these means. Note that although mode jumps appear as steps in the beat frequency $f(t)$ during the first part of the filling stage [panel (a) in Fig. 8], when the changes in cavity mode numbers displayed in panel (b) [i.e. the $\Delta m_m(t)$ and $\Delta m_r(t)$] are taken into account, the shift in the unwrapped beat frequency, $\Delta f_{UW}(t)$, illustrated in panel (c), as well as the assessed pressure, shown in Fig. 9, are almost fully continuous functions with solely a few minor "kinks" during the initial part of the gas filling stage. Since the evaluation procedure is not using data points during this part of the filling stage, they do not affect the final assessments.

A more detailed scrutiny of the transient behavior of the assessed beat frequency, i.e. $\Delta f_{UW}(t)$, is displayed in Rubin et al. [48]. It is there shown that $\Delta f_{UW}(t)$ takes its steady-state value within a fraction of the gas filling part of the modulation cycle, typically within 10 s after the end of the t_f-period of the gas filling part of the gas modulation cycle.

7 Achievements of GAMOR

An important prerequisite for a measurement system exhibiting a small amount of uncertainty is to provide a high degree of precision. As is described above, the main feature of the GAMOR method is to reduce the influence of disturbances, primarily fluctuations and drifts. It is an indisputable fact that this leads to a high degree of precision. To assess to which extent the GAMOR methodology is capable of doing this, this was therefore one of the first objectives during the early development of the GAMOR methodology.

Following some first demonstrations of the ability of the methodology to improve on precision in both non-temperature stabilized [41] and temperature stabilized [42] systems, a pair of experimental verification of the predicted abilities of the GAMOR methodology to mitigate the influence of fluctuations [43] and drifts [44] were performed.[21] Work was then performed regarding assessment of the precision of the Invar-based DFPC system utilizing the GAMOR methodology [45, 46]. Two Invar-based DFPC GAMOR-utilizing systems were then assessed for their mutual short-term ability to assess pressure [47].

Following this development, a series of works were then performed, all as a part of the "QuantumPascal" project, to make possible assessments of various physical entities with low uncertainty, addressing concepts such as the influence of thermodynamic effect associated with the filling and emptying of the measurement cavity in the Invar-based DFPC GAMOR system, i.e., pV-work [48, 49], means to measure the gas temperature [46, 48], and development of disturbance-resistant methodologies for assessment of cavity deformation [50] and accurate in-situ assessment of the penetration depth of mirrors comprising a quarter-wave stack (QWS) reflection coating of type H [51]. In addition to this, an assessment of the extended uncertainty of the Invar-based system was performed [52].

Based on these developments it was then possible, largely within the "QuantumPascal" project, to develop transportable refractometer systems that can be used to compare pressure assessing systems at various NMIs [47, 52–54].

The results of the development of the GAMOR methodology during the last years have recently been summarized by various review papers, one published in *Acta IMEKO* regarding recent advances in Fabry-Perot-based refractometry utilizing gas modulation for assessment of pressure [55], an invited review published in *Spechrochimica Acta B* focused on the ability of the methodology to assess molar density [56], another, likewise invited, addressing the assessment of pressure, published as a topical review in an special issue of the journal *Journal of Optics* focusing on scientific achievements in the

[21] While the works [41–43] were performed before the initiation of the "QuantumPascal" project, a majority of the works were done as a part of it, viz. [44–58]

field of optics in Sweden [57], and finally a fourth describing the progress of the entire Quantumpascal project in Acta IMEKO [58].

7.1 Experimental verification of the predicted abilities of the GAMOR methodology to mitigate the influence of disturbances

In order to be able to develop refractometry towards improved performance, it is of importance to verify the theoretical predictions of the abilities of the GAMOR methodology to automatically mitigate the influence of fluctuations and drifts that were predicted in the sections 4.1 and 4.2 above. Experimental investigations of these abilities have therefore been performed.

7.1.1 Verification of the predicted ability of GAMOR to reduce the influence of fluctuations

To experimentally verify the predictions of the model for reduction of the influence of fluctuations from above, which states that the length of the gas modulation cycle plays a significant role in mitigating the influence of fluctuations in the system [43], measurements were performed under a given (typical) set of conditions but evaluated for different cycle lengths. Figure (10) shows the standard deviation of a 50 h long series of measurements of an empty measurement cavity evaluated in eight different ways, corresponding to gas modulation periods, t_{mod}, ranging from 100 s to 30,000 (8.3 h), as a function of the gas modulation period.

The figure shows that the standard deviation decreases markedly with decreased modulation period; in this particular case, more than 50 times (from 50 to 0.9 mPa) as the length of the modulation cycle is decreased from 30,000 to 100 s. This confirms the predictions given in section 4.1 about the ability of GAMOR to reduce the influence of fluctuations.

To further confirm the alleged advantage of short gas modulation periods, and also illustrate the importance of assessing measured quantities as averages over a multitude of modulation cycles, Fig. (11) displays the Allan deviations of the data displayed in Fig. (10) with the three shortest gas modulation periods [100 s (the lowermost curve), 300 s, and 500 s (the uppermost)] as functions of averaging time.

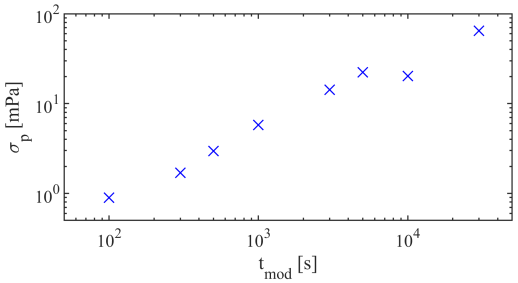

Figure 10. Standard deviation of a 50 h long series of measurements of an empty measurement cavity evaluated in eight different ways, corresponding to gas modulation periods, t_{mod}, ranging from 100 to 30,000 s, as a function of the length the gas modulation cycle. Reproduced with permission from Ref. [43].

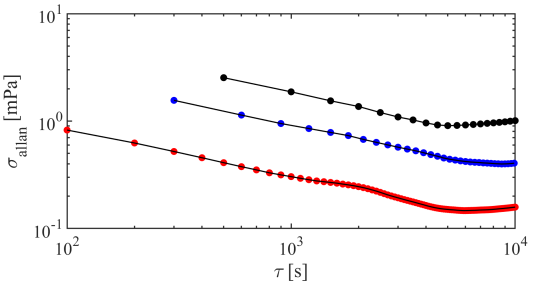

Figure 11. Allan deviations of the data representing the three shortest gas modulation cycle times in Fig. 4, viz., 100 s (lowermost, red markers), 300 s (blue markers), and 500 s (uppermost, black markers) as a function of averaging time. Reproduced with permission from Ref. [43]

In agreement with the data shown in Fig. (10), Fig. (11) shows that the Allan deviation of the shortest gas modulation period (100 s) is consistently smaller than those of the other cycle lengths. The data also display that the deviation depends on the averaging time. For averaging up to around a few thousand seconds, it decreases monotonically with averaging time (with a white-noise dependence); from 0.9 mPa, which it takes when there is no averaging, thus for a series of individual modulation cycles (each being 100 s), down to 0.15 mPa, which it takes for an averaging of 60 cycles (to an averaging time of 6000 s). This thus shows that the influence of disturbances can additionally be reduced by aver-

aging over a number of gas modulation cycles.

The data displayed in Fig. (11) also show that for longer averaging times, above 5 000 - 10 000 s (i.e. 1.5 - 3 h), the Allan deviation levels off and starts to increase with averaging time. This indicates that the system starts to be affected by drifts. The reason why the data are not affected by drifts until such considerable times as one or three hours is that the gas modulation procedure does not only reduce the influence of fluctuations but also drifts.

These measurements do not only verify the predictions of the model regarding the ability of gas modulation to, in an automatic manner, mitigate the influence of fluctuations given in Ref. [43], but also the alleged assumption that a rapid gas modulation process, which is one of the cornerstones on which the GAMOR methodology relies, is highly beneficial for refractometry.

7.1.2 Verification of the predicted ability of GAMOR to reduce the influence of drifts

To experimentally verify the predictions of the model for the reduction of drifts from above, e.g. the Eqs (16) - (17), a set of measurements were made that was deliberately affected by drifts, viz. by use of a system not in thermal equilibrium.[22]

Measurements were taken from the Invar-based refractometry system described in this guide as well as elsewhere [45] with the measurement cavity being constantly evacuated while the temperature of the cavity spacer was increased from room temperature (23 °C) to the melting temperature of Ga (29.76 °C). As a result of this, the length of both cavities increased monotonically during this process.[23]

Figure (12) shows the error the system makes in the assessment of refractivity (expressed in terms of the corresponding pressure) as a function of the length of the gas modulation cycle (for cycle lengths ranging from 100 to 51 200 s) in the absence and presence of interpolation (by the uppermost and lowermost curve, respectively) [44].

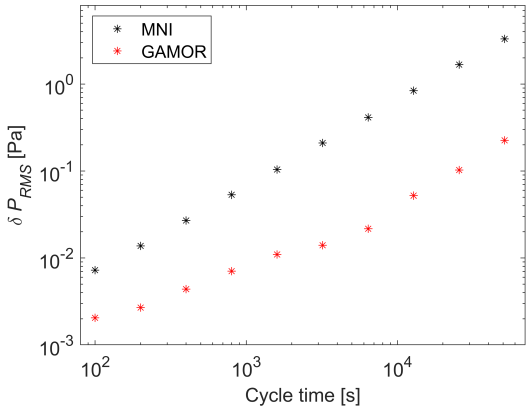

Figure 12. The error in the assessment of pressure as a function of the length of the modulation cycle of the Invar-based refractometry system when its temperature was increased from room temperature (23 °C) to the melting temperature of Ga (29.76 °C), evaluated by non-interpolated and interpolated (i.e. GAMOR) refractometry (the uppermost and lowermost data sets, respectively). Reproduced with permission from Ref. [44]

The data show first of all that the error in the assessment decreases significantly with decreased length of the gas modulation cycle, for the unmodulated case, from 3.3 Pa (for a gas modulation cycle length of 51 200 s) to 7 mPa (for a length of 100 s). The lower set of data (ranging from 0.2 Pa to 2 mPa) represents the corresponding cases for the GAMOR methodology.

These data then also indicate that the uncertainties in the assessments are consistently lower when interpolation is utilized (in the figure denoted GAMOR) than when non-interpolated methodologies (denoted MNI) are used.

These behaviors are in full agreement with the model presented in section 4.2, and thus verify its predictions; it also illustrates clearly the advantage of GAMOR (represented by the leftmost red data point in the lower set of data, 2 mPa) over conventional unmodulated non-interpolated refractometry (represented by the rightmost black data point in the upper set of data, 3.3 Pa) regarding the ability to re-

[22] This does not imply that the abilities of the various methodologies addressed to mitigate the influence of drift only appear (or are of importance) in systems with significant amounts of drift; on the contrary, they take place also in well-stabilized systems with less amounts of drifts.

[23] Since the changes in length of the two cavities were not identical (the heating process affected the two cavities in a slightly dissimilar manner), the beat frequency between the two laser fields drifted over time.

duce the pick-up of drifts.

7.2 Demonstration of the ability of the GAMOR methodology to improve on precision

It has repeatedly been shown that the GAMOR methodology has an outstanding ability to reduce the influence of fluctuations and drifts on the assessments of refractivity to such an extent that the precision of the assessments can be significantly improved. The extent to which the methodology is capable of mitigating disturbances has therefore been scrutinized under a variety of conditions.

7.2.1 Ability of GAMOR to reduce the influence of drifts from a non-temperature stabilized system

As a part of a previous EMPIR project (JRP 14IND06 'Pres2Vac'), it was demonstrated that the GAMOR methodology, when applied to a DFPC refractometer utilizing a non-temperature-stabilized cavity spacer made of Zerodur, could reduce the influence of drifts more than 3 orders of magnitude (decreasing the standard deviation of a given set of assessments from 6.4 Pa to 3.5 mPa) [41].

The data in Fig. (13) show, by panel (a), that, while the temperature drifts 250 mK over a period of 24 h (uppermost curve, blue in color, right axis), the pressure assessed by ordinary single FP cavity refractometry drifts 20 Pa (lowermost curve, red in color, left axis). The pressure assessed by the GAMOR methodology (middle curve, black in color, left axis) does not show any fluctuations on the given scale (± 15 Pa). Panel (b) though, which displays the pressure assessed by the GAMOR methodology on an enlarged scale (± 5 mPa), shows that the refractometer, when the GAMOR methodology was used, solely picked up disturbances on the low mPa scale (with a 2σ of 3 mPa).

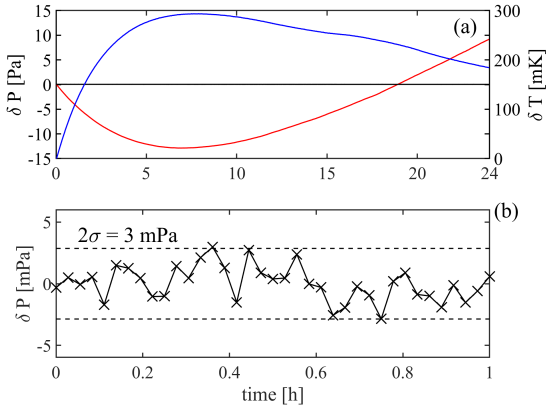

Figure 13. Panel (a): A 24 h long series of measurement of an empty measurement cavity evaluated by two different means: the lowermost curve (red in color) - without gas modulation, referred to as a static mode of detection, and the almost fully horizontal curve (black in color) - by use of the GAMOR methodology (both left axis). The uppermost curve (blue in color and right axis) represents the temperature. Panel (b): a zoom in of the first hour section of the data taken with the GAMOR methodology. Reproduced with permission from Ref. [41]

7.2.2 An alternative realization of GAMOR— Gas-equilibration GAMOR (GEq-GAMOR)

The GAMOR methodology can, in fact, be carried out in several ways. In contrast to the conventional one, described above, in which the measurement cavity is repeatedly filled and emptied with gas while the reference cavity is held at a constant pressure, at vacuum, denoted single cavity modulated GAMOR (SCM-GAMOR), it was demonstrated, also as a part of the previous EMPIR project "Pres2Vac", that it is alternatively possible, instead of evacuating the measurement cavity, to equilibrate the pressure in the two cavities. The alleged advantage of this methodology, which goes under the name Gas-equilibration GAMOR (GEq-GAMOR), is that the time it takes to obtain adequate conditions for the reference measurements can be shortened, whereby more time can be spent on the averaging of data when there is gas in the measurement cavity [42].

As is shown in Fig. (14), using this methodology, addressing a pressure of N_2 of 4303 Pa inside a temperature stabilized Zerodur cavity, a sub-ppm (1σ) precision (i.e. < 4 mPa) could be demonstrated. More specifically, it was shown that the system (the red curve, the third set of data counted from above) could provide a response for short integration times (up to 10 min) of 1.5 mPa $(\text{cycle})^{(1/2)}$,

while for longer integration times (up to 18 h), it showed an integration time-independent Allan deviation of 1 mPa (corresponding to a precision, defined as twice the Allan deviation, of 0.5 ppm), exceeding the performance of the SCM-GAMOR methodology (the blue curve, the uppermost set of data) by a factor of 2 and 8, respectively [42].

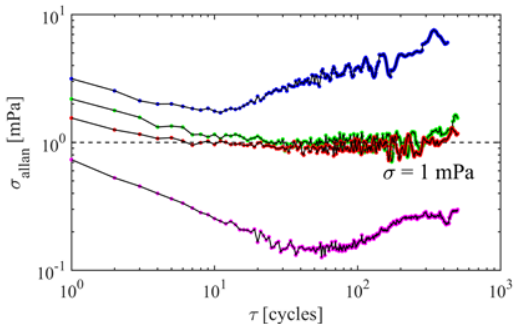

Figure 14. Allan deviations, σ_{Allan}, of data taken from a temperature regulated DFPC made of Zerodur: Blue markers (uppermost set of data): ordinary single cavity modulated GAMOR (SCM-GAMOR) [41], and red markers (third set of data counted from above): GEq-GAMOR, both taken for a set pressure of 4303 Pa. Green markers (the second set of data) represent the GEq-GAMOR data evaluated with a reduced integration time of the residual gas pressure measurement (see [42] for details). The violet markers (lowermost set of data): GEq-GAMOR, zero pressure measurement. Dashed line: an Allan deviation of 1 mPa. Reproduced with permission from Ref. [42]

Since the GEq-GAMOR methodology could be performed with averaging times of 40 s while the ordinary SCM-GAMOR methodology utilized 10 s, this methodology demonstrated performance similar to expectations [a reduction of the white noise response by a factory of 2, given by $\sqrt{(40/10)}$].

Partly based on these two early GAMOR works [41, 42], the 'Pres2Vac' project produced recommendations for the use of gas modulated optical based methods for "assessments of absolute, positive and negative pressures in the 1 Pa to 10^4 Pa range", both with regard to their use and a requirement of further research and development to reach the full potential of the technique in the longer term.

7.2.3 Assessment of precision of the Invar-based DFPC system utilizing the GAMOR methodology

The GAMOR methodology has not only provided a means to reduce the influence of disturbance on the assessment of refractivity, which has improved the precision of assessments, it has also provided a variety of means to improve on the instrumentation. One such is that it opens up for the use of non-conventional cavity-spacer materials, e.g. Invar. As was shown in Fig. 5, a GAMOR-based system based on an Invar-FPC, shortly described in section 5.2 above, has therefore been realized and characterized [45, 46]. As is shown below, this system has demonstrated a number of appealing properties.

The most prominent reasons why Invar can be seen as an appealing material for refractometry are the following ones [45, 46]:

(i) Invar has a *high volumetric heat capacity*. This implies that a given amount of energy (supplied by the gas) only provides a small temperature increase in the spacer material;

(ii) It has a *high thermal conductivity*. This implies that any possible small temperature inhomogeneity created by the filling or evacuation of gas will rapidly spread in the system (faster than in systems with cavity spacers made of glass materials) so as to make the temperature of the DFPC-system homogeneous in a short time, which is a prerequisite for an accurate assessment of the temperature of the gas when using short modulation cycles;

(iii) It has *a high Young's modulus*, which gives the cavity a lower pressure induced deformation;

(iv) It has a *low degree of He diffusivity and permeation*, significantly lower than that of ULE glass. This implies that there are virtually no memory effects when He is addressed; and

(v) Invar can be *machined in a standard metal workshop*. This implies that more complicate geometries can be created swiftly and to a low cost.

This has allowed Invar-based FPC-systems to be constructed with a number of appealing features, e.g.:

(vi) The cavity system can be made "*closed*". This implies that the gas does not fill a volume surrounding the spacer as is the case for an "open" system; instead it fills only one of the cavities. This restricts the amount of gas being transferred into the refractometer in a single gas filling cycle;

(vii) Each cavity can be manufactured with a *narrow bore* (with a radius of 3 mm). This implies that the gas rapidly takes the temperature of the cavity wall (within a fraction of a second) and that each filling of gas brings in only a small volume of gas (with a spacer length of 148 mm, < 5 cm^3), and thereby, when 100 kPa is addressed, only a small amount of energy (< 0.5 J), so as to reduce the amount of pV-work;

(viii) The system can be constructed *without any heat islands* (i.e. regions that are connected with low thermal conductance), which additionally adds to the ability that a small temperature inhomogeneity created by the filling or evacuation of gas will rapidly spread in the system so as to make the temperature of the DFPC-system homogeneous in a short time; and

(ix) *The temperature of the cavity spacer* can be assessed by the use of sensors either placed in holes drilled into the cavity spacer (three Pt-100) or wrapped around the outside of the spacer (a thermocouple) whose output is *referred to a gallium fix point cell.* This implies that the assessment of gas temperature is not affected by any possible homogeneous heating of the cavity spacer; it is only influenced by the difference in temperature between the cavity spacer at the position(s) of the sensors and that of the cavity wall.

Based on this, as was shown in Fig. 5, a GAMOR-utilizing system based on an Invar-based DFPC refractometer, has therefore been realized and characterized [52, 45, 46]. Utilizing this instrumentation, together with a DWPG to provide a reference pressure, it has been demonstrated that it can outperform earlier systems based on Zerodur® and provide assessments with sub-ppm precision. Figure (15) shows a set of uninterrupted measurement data taken over 24 h by the Invar-based DFPC instrumentation, presented as the difference, ΔP, between the pressure measured by the refractometer, P, assessed from the Eqs. (10) - (15) using molecular parameter values from [41], corrected by a deformation independent correction term ψ, and the estimated set-pressure of the DWPG, P_{Set}, for an empty measurement cavity and one at a pressure of 4303 Pa [50].

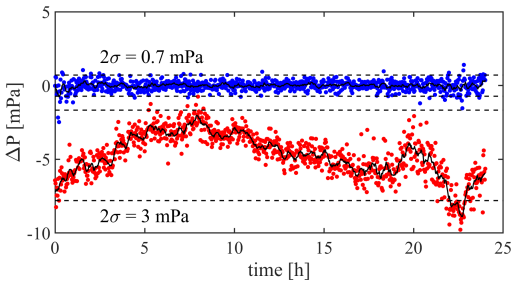

Figure 15. The difference between the pressure of nitrogen assessed by the refractometer (corrected, according to Ref. [50] by a deformation-independent correction term, denoted ψ), P, and the estimated pressure supplied to the refractometer, P_{Set}, denoted ΔP, for an empty cavity (blue set of data) and at a pressure of 4303 Pa (red set of data), respectively. The black curves represent moving averages of 10 samples. The dashed lines correspond to $\pm$ 2σ of the assessed pressure difference. Reproduced with permission from Ref. [45].

The data show, over a period of 24 h, for the empty measurement cavity data (the upper set of data, blue in color), a $\pm 2\sigma$ spread of 0.7 mPa (corresponding to spreads in refractivity and beat frequency of 2×10^{-12} and 370 Hz, respectively). For 4303 Pa (the lower set of data, red in color), the data have a spread of 3 mPa (0.7 ppm) and a mean deviation of -4.7 mPa (1.1 ppm).

Although the lower curve in Fig. (15) shows a noticeable amount of fluctuations, it is worth to note that the precision of the data is, in fact, excellent. This is presented, for illustrative purposes, by Fig. (16), which displays, as a function of time, this GAMOR data in seven separate panels, (a) – (g), with successively enlarged scales of the y-axis. While panel (a) displays the signal with a y-scale ranging over 8 kPa, the subsequent panels (b) – (g) display the same data with successively one order of magnitude smaller range of the y-axis: i.e., 800 Pa, 80 Pa,

8 Pa, 0.8 Pa, 0.08 Pa and 0.008 Pa, respectively. Each red data point represents an individual GAMOR cycle, while the black, dashed curves represent moving averages of 10 cycles.

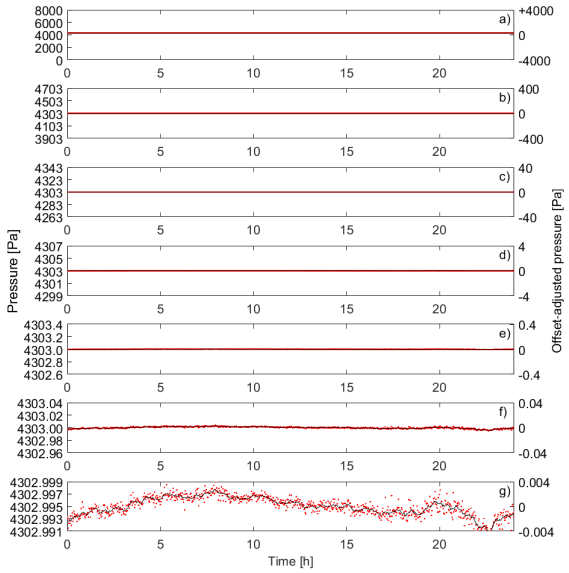

Figure 16. The GAMOR signal from 4303 Pa of nitrogen measured over 24 hours. The various panels (a) – (g) display the same set of data with successively smaller scales of the y-axis. Left axis: Pressure; Right axis: Offset-adjusted pressure. Panel (a) displays the response with an y-axis scale of 8 000 Pa while the subsequent panels (b) – (g) display the same data with successively one order of magnitude smaller range of the y-axis: i.e., the panels (b) – (g) cover 800 Pa, 80 Pa, 8 Pa, 0.8 Pa, 0.08 Pa and 0.008 Pa, respectively. Hence, panel (g) is an enlargement of panel (a) by six orders of magnitude. Each red data point represents an individual GAMOR cycle. The black, dashed curves represent moving averages of 10 cycles. Reproduced with permission from Ref. [56]

To analyze this data in more detail, Fig. (17) displays a comparison between the Allan deviations of the GAMOR data from the Invar-based system presented in Fig. (15) (given by the blue and red markers) and a system with a Zerodur spacer (green markers [42]).

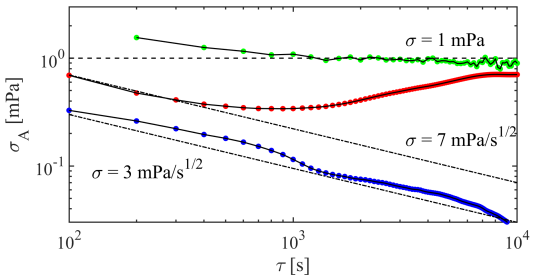

Figure 17. Allan deviations, σ_A, of pressure assessments made by the GAMOR methodology. Green markers: data earlier obtained at 4303 Pa from a Zerodur cavity [42]; Red markers: data taken at the same pressure by the Invar-based system presented in [45]; Blue markers: data taken by the Invar-based system with an empty measurement cavity; Dashed horizontal line: an Allan deviation of 1 mPa; Dash-dotted slanting lines: Allan deviations corresponding to a white noise level of 7 and 3 mPa s$^{1/2}$, respectively. Reproduced with permission from Ref. [45].

This data show, as is expected of GAMOR, which is insensitive to long-term drifts of the cavity length, that the Allan deviation of data taken from an empty cavity (in which temperature drifts become irrelevant) does not show any noticeable drift (lowermost curve, blue in Fig. 17); such measurements are solely limited by white noise, in this case at a level of 3 mPa s$^{1/2}$, providing a minimum deviation of 0.03 mPa (which corresponds to a deviation of the detected beat frequency of 16 Hz) at 10^4 s. This shows, in accordance with assumptions and predictions, that the system, within these measurement times, only picks-up minute amounts of fluctuations or drifts from an empty measurement cavity assessment.

The data taken at 4303 Pa (red markers), on the other hand, show, for measurement times up to 500 s, a slightly higher white noise level of 7 mPa s$^{1/2}$, after which flicker noise or drifts affect the system.

This implies that the 0.7 ppm spread in the lowermost curve in the Fig. (15) is mainly attributed to drifts in the temperature assessments and of a pressure gauge in the system. The mean deviation between the pressure measured by the refractometer and the set-pressure of the pressure balance at 4303 Pa of 1.1 ppm originates mainly from drifts in the temperature assessments between the instants of

characterization and measurements.

This is a clear improvement from previous assessments based on a Zerodur cavity for which the white noise levels of the empty cavity measurement and that at 4303 Pa were 10 and 22 mPa $s^{1/2}$, respectively (where the latter are displayed by the green markers in Fig. 17) [42].

The Allan plot analysis shows that the optimum integration time for assessment of 4303 Pa was around 1000 s (corresponding to 10 modulation cycles). Under these conditions, the system demonstrated a minimum (Allan) deviation of 0.34 mPa [which corresponds to relative deviation (or 1σ precision) of 0.08 ppm] [45]. For longer integration times, the deviation increased (attributed to fluctuations in the temperature measurement module) before it reached a plateau of 0.7 mPa (at 7 000 s).

The minimum level of deviation of the system was found to be significantly better, and that of the plateau slightly better, than the 0.9 - 1 mPa reached with the Zerodur cavity [42].

7.2.4 Short-term performance of two Invar-based DFPC GAMOR systems for assessment of pressure

There is a number of applications, e.g., characterization of pressure sensors and studies of rapidly changing pressures or processes giving rise to such, for which it is of importance that the system has a fast response. Although several types of refractometers have been scrutinized over the years [13–22, 30, 41, 42, 45, 46, 50, 52, 53, 55], none of them has yet been characterized with respect to its short-term behavior. It is therefore of importance to perform such characterizations. By use of two GAMOR based systems (of which one is the transportable, denoted the "Transportable Optical Pascal", abbreviated the TOP, described below), it has been demonstrated that the combination of Invar-based FPC and the GAMOR methodology is suitable also for assessments of pressure shifts with short settling times.

As is shown in Fig. (18), by connecting the aforementioned stationary and the transportable GAMOR-based refractometry systems (where the former is denoted the "Stationary Optical Pascal", i.e. the SOP) to the same gas system, whose pressure was set by a common DWPG, their short-term performances could be scrutinized in some detail [47]. As the refractometers were independent, it could be concluded that deviations that are common to both systems are not inherent to any of the refractometers, but rather to the DWPG or the gas handling system. Thereby, by addressing their common response (in reality, the difference between them), it was possible to assess the short-term performances of two independent GAMOR-utilizing refractometers regarding their ability to assess pressure without any influence from the DWPG or the gas handling system.

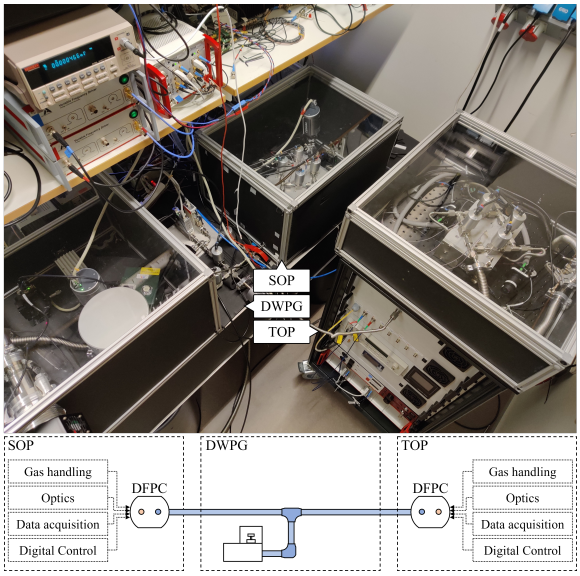

Figure 18. The SOP (the stationary optical Pascal) system (in the rightmost box on the optical table) and the TOP (the transportable optical Pascal) system (to the right), both connected to a common DWPG (in the leftmost box on the optical table), gas supply (between the SOP- and DWPG boxes), vacuum system (not in the figure), and computer (for control and data acquisition), together with various electronics (for the SOP, partly seen on the shelves, and, for the TOP, in the rack). The bottom part of the figure shows a schematic illustration of the two refractometers and their connection to the DWPG. Reproduced with permission from Ref. [47]

Figure (19) shows, in panel (a), an enlargement of 70 s of refractometry data taken by the SOP and the TOP from 16 kPa of N_2 generated by a common DWPG. Panel (b) displays the same data in a correlation plot. The latter plot shows that the refrac-

tometers can provide a short-term precision on the 1 s time scale of 3×10^{-8}, which is one order of magnitude better than the corresponding stability of the pressure provided by the DWPG. This illustrates that the stability of such an assessment is not primarily limited by the refractometer. This opens up for a number of novel applications for refractometry.

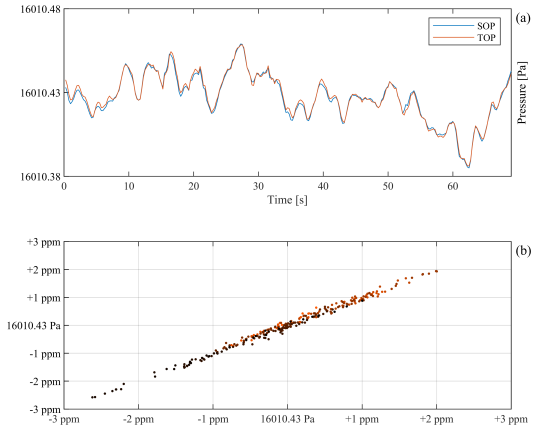

Figure 19. Panel a): an enlargement of 70 s of refractometry data taken by the SOP and the TOP from 16 kPa of N_2 generated by a common DWPG. Panel b): A correlation plot of the same data. In the latter panel, the x- and the y-axes represent the pressures assessed by the SOP and the TOP, respectively. Time is represented by the color, where the first data points are marked with orange color while the last ones are in black. Reproduced with permission from Ref. [47]

7.3 Demonstration of the ability of GAMOR-based refractometer systems to provide low uncertainty assessments

To properly assess pressure, and, in particular, if a primary standard is to be realized, it is of importance to not only have an outstanding precision, it is also necessary to certify that the assessments can be made with low enough uncertainty. To be able to achieve this, there are a number of issues that need to be addressed adequately in order for a GAMOR-based refractometer system to provide low uncertainty assessments. Of special importance are the influence of thermodynamic effects on the assessments (i.e., pV-work) [48, 49], the ability to properly and accurately assess the gas temperature [46, 48], and assessment of to which extent pressure induced cavity deformation [50], mirror penetration depths [51], and the Gouy phase [51] affects assessments. To address the concept of accuracy, so as to be able to assess the total uncertainty of a pressure assessment, the influences of these concepts on the assessment of pressure by use of the Invar-based DFPC system have been addressed in some detail in a number of separate works [46, 48–51].

7.3.1 The influence of thermodynamic effects (pV-work) on the assessments and the ability to assess gas temperature accurately

To accurately assess pressure, it is vital to certify that the assessments are not affected by any thermodynamic effects from the gas filling and emptying processes, i.e., pV-work, and to assess the temperature of the gas accurately. The aforementioned features of the GAMOR methodology (given in the sections 7.1 and 7.2) provide a number of properties of the system that vouch for both virtually no influence of any pV-work and a good ability to assess gas temperature.

A recent work by Rubin et al. was dedicated to a scrutiny of to which extent the Invar-based DFPC system is affected by pV-work when the GAMOR methodology is applied [48].

Simulations of gas dynamics showed, among other things, that, primarily due to the "reasons" (vi) and (vii) given in section 7.2.3, i.e. that the system is "closed" and that each cavity has been manufactured with a narrow bore (with a radius of 3 mm), the equilibration of pressure in the cavity when nitrogen is let in takes place on a time scale of ten milliseconds and that the gas adopts the temperature of the cavity wall on a time scale of less than a couple of seconds [48].

Simulations of the transfer of heat in the system were used to estimate the characteristic time scale for the heat dissipation process. This was assessed to be in the few or ten second range. The cause for this is, in addition to the "reasons" (vi) and (vii) from above, also (i), (ii), and (viii), which state that Invar has a high volumetric heat capacity, a high thermal conductivity, and that it has been possible to con-

struct the system without any heat islands. Additionally, as indicated by "reason" (vii), since the cavity volume is small (< 5 cm^3), the gas transfers only a small amount of energy (< 0.5 J) into the system during a gas filling process. Due to the high heat capacity of Invar, this will give rise to only a minor local heating of the cavity spacer. In addition, due to the large thermal conductivity of Invar (one order of magnitude larger than for typical glasses) and since the system is constructed without heat islands, this minor local heating will rapidly dissipate into the material and provide a small homogeneous change in temperature of the entire spacer block (in the order of 0.3 mK) [48].

When gas is evacuated from the cavity during the second part of the modulation cycle, a similar amount of energy is removed from the system, giving rise to a similarly sized temperature decrease of the system. The net supply of energy to the cavity from the gas filling and emptying process is therefore practically negligible [48].

Moreover, since the system assesses temperature by the use of sensors placed either in holes drilled in the cavity spacer or wrapped tightly around the outside of the spacer, any possible homogeneous heating of the cavity spacer can be measured and will directly be accounted for. Therefore, the pressure assessments are only influenced by the difference between the temperature of the cavity walls and that of the cavity spacer at the position(s) of the sensors. It was found that, under normal conditions (for pressures up to 100 kPa and when the gas modulation periods are 100 or 200 s), this difference will, when the refractivity assessments are made, be minute, well into the sub-mK range [48].

It was estimated in that work that an upper limit for the influence of pV-work made by nitrogen on the Invar-based DFPC system, is, for 100 s long modulation cycles, 0.5 mK/100 kPa (or 1.8 ppm/100 kPa) and, for 200 s long cycles, 0.4 mK/100 kPa (or 1.3 ppm/100 kPa) [48].

These estimates were compared with experiments. Since none of these assessment performed in the 4 - 30 kPa range in Ref. [48] showed any resolvable effect from pV-work, they support the estimates. A subsequent study addressing 100 kPa was able though to detect a minor influence of pV-work on the assessments [49]; it was found that the heating of the cavity spacer in reality is significantly lower than the upper limits predicted by the simulations; the measured temperature deviations were found to be about one third of those. This suggests that, for the cases of 100 and 200 s long modulation cycles, deviations of 0.16 and 0.12 mK/100 kPa, corresponding to sub-ppm levels/100 kPa, should prevail, respectively.

This implies that the Invar-based DFPC system utilizing the GAMOR methodology is not expected to be significantly affected by thermodynamic processes that are associated with the exchange of gas (i.e., pV-work). Such effects are therefore currently not a limiting factor when the Invar-based DFPC GAMOR system is used for assessments of pressure or if it would be used as a primary pressure standard, up to atmospheric pressure.

7.3.2 Development of a Ga fixed-temperature cell for accurate assessment of temperature.

As is shown by Silander et al. [46], to properly assess the temperature of the spacer block of the Invar-based DFPC refractometer, it was equipped with an automated, miniaturized gallium fixed-point cell. Utilizing repeated heating-and-cooling cycles, where each heating part, which serves as the reference to thermocouple sensor, lasts ca. 100 h.

As is described in some detail in the guide "*Development of methods for control and assessment of the temperature of the gas in Fabry-Pérot cavities*" [67], it was found that, during the most stable part of the Ga melting cycle, the combined ($\pm\ 2\sigma$) stability of the fixed-point cell and thermocouple measurement was smaller than 220 μK. An estimate of the total uncertainty in the temperature measurement system indicated 1.2 mK (4 ppm), dominated by the stability of the nanovoltmeter used for assessment of the thermocouple voltage [46].

7.3.3 Development of a disturbance-resistant methodology for assessment of cavity deformation

The high precision has also allowed for the realization of a novel, disturbance-resistant methodology for assessment of cavity deformation in FPC refractometers [50]. It is based on scrutinizing the difference between two pressures: one assessed by the uncharacterized refractometer and the other provided

by an external pressure reference system, at a series of (set) pressures for two gases with dissimilar refractivity, He and N_2.

By fitting linear functions to these responses and extracting their slopes, two physical entities of importance could be constructed: one representing the cavity deformation (more precisely, the refractivity-normalized relative difference in the change in lengths of the two cavities due to pressurization), in this work denoted ε', and the other comprising a combination of the systematic errors of a multitude of physical entities, ψ, (those of the assessed temperature, the molar polarizabilities, and the set pressure). This provides a robust assessment of cavity deformation with small amounts of uncertainties [50].

A thorough mathematical description of the procedure served as a basis for an evaluation of the basic properties and features of the procedure [50]. This indicated that the cavity deformation assessments are independent of systematic errors in both the reference pressure and the assessment of gas temperature, and when the GAMOR methodology is used, that they are insensitive to gas leakages and outgassing into the system.

It has been shown that when a high-precision (sub-ppm) refractometer is characterized according to the procedure, and under the condition that high purity gases are used, the uncertainty in the deformation contributes to the uncertainty in the assessment of pressure of nitrogen on a level of 1 or 2 ppm (depending on which type of N_2 pressure standard it refers to; a mechanical or a thermodynamic one, respectively) [52]. Since this presently solely is a fraction of the uncertainty of the molar polarizability of nitrogen, this implies that, in practice, as long as gas purity can be sustained, cavity deformation is not a limiting factor in FP-based refractometer assessments of pressure of nitrogen.

7.3.4 Development of a methodology for accurate in-situ assessment of the penetration depth of mirrors comprising a quarter-wave stack (QWS) high-reflection coating of type H

An experimental methodology for assessment of the influence of the penetration depth of QWS mirror coatings of type H on the assessment of refractivity, for the case when the laser is centered on the mirror design frequency, through the γ_c entity, defined in close proximity to the Eqs. (2) and (3), and, when the mirrors are not used around their center frequency, the γ_s' entity, was developed and presented by Silander et al. [51]. The procedure encompasses accurate assessments of the FSR, measured by the use of induced mode jumps and the frequency of the empty cavity mode, ν_0, assessed by referencing the locked laser to an optical frequency comb, together with the use of the mode number, m_0, which, since it is an integer, can be assessed without uncertainty.

Using the presented methodology, the γ_s' entity for the mirrors addressed could be assessed, under the same conditions as when refractivity measurements are performed and without modifying the set-up, with a relative uncertainty of 2% [to 1.728(32)]. This implies that the mirror coatings will not significantly influence the uncertainty of assessments of refractivity and pressure; they contribute to the expanded uncertainties of these entities with contributions that solely are $< 8 \times 10^{-13}$ and (for nitrogen) < 0.3 mPa, respectively [51]. This implies that the methodology is suitable for elimination of the influence of penetration depth of QWS coated mirrors of type H in FP-based refractometry.

7.3.5 Assessment of the uncertainty of the stationary and the transportable Invar-based FPC optical Pascals — the SOP and the TOP — for assessment of pressure

The two Invar-based FPC systems utilizing the GAMOR methodology described above (the Stationary and Transportable Optical Pascals, denoted the SOP and the TOP) were characterized with respect to their abilities to assess pressure in the 4 - 25 kPa range [52].

Based on the fact that the influence of thermodynamic effects on the assessments (i.e., the pV-work) can be neglected [48], that the construction allows for low uncertainty assessments of gas temperature [46], and that the pressure induced cavity deformation could be assessed with low uncertainty [50], and assuming that the influence of the mirror penetration depth and the Gouy phase could be neglected [51], the expanded uncertainty of the two

refractometers could be assessed to [52]:[24]

- for the SOP: $[(10\ \text{mPa})^2 + (10 \times 10^{-6} P)^2]^{1/2}$;
- for the TOP: $[(16\ \text{mPa})^2 + (28 \times 10^{-6} P)^2]^{1/2}$.

It was concluded that while the uncertainty of the SOP is mainly limited by the uncertainty in the molar polarizability of N_2 (8 ppm), that of the TOP is limited by the temperature assessment (26 ppm) [52].

To verify the long term stability, the systems were also compared to each other over a period of 5 months. It was found that all measurements fell within the estimated expanded uncertainty (k=2) for comparative measurements (27 ppm). This verified that the estimated error budget for the uncorrelated errors holds over this extensive period of time.

7.4 Realization of transportable refractometer systems based on the GAMOR methodology

The ability of the GAMOR methodology to mitigate the influence of fluctuations and drifts has also enabled the realisation of transportable refractometry systems. A first version was realized as a part of the previous EMPIR project (JRP 14IND06 'Pres2Vac') although its performance was assessed as a part of the present "QuantumPascal" project [53]. Its functionality was demonstrated at the last workshop at the National Metrology Institute at RISE, in Borås, Sweden, 2018 with sub-ppm precision (0.5 – 0.9 ppm). The system was thereafter disassembled, packed and transported on winter roads in sub zero °C temperature 1 040 km to Umeå University, where it, after unpacking and reassembling, demonstrated a similar precision (0.8 – 2.1 ppm). This shows that the system could be disassembled, packed, transported, unpacked, and reassembled with virtually unchanged performance [53].

[24] Since the mirror penetration depth and the Gouy phase were neglected in the work by Silander et al. [52], the analysis was based on Eq. (4) above, which, according to footnote 3, is based on a cavity resonance condition given in terms of the number of wavelengths the light experiences under a round trip. As is discussed in the proximity of Eq. (9), this is adequate as long as the empty measurement cavity frequency is defined as an "effective" empty cavity frequency, ν_0', given by $\nu_0/(1+\frac{\Theta_G}{\pi m_0}+\frac{\gamma_c'}{m_0})$. This was not done within the work by Silander et al. [51] though. However, as is discussed in footnote 29 of Silander et al. [51], although this implies that the cavity mode number was incorrectly assessed by Silander et al. [52] by a single unit, when this redefinition is included in the analysis, it does not affect the assessment of the uncertainty of the instrumentation.

Based on this successful realization, and addressing its identified shortcomings, a second version of a transportable refractometer system, the TOP, was constructed as a part of the present EMPIR JRP project, 18SIB04 "QuantumPascal" As is shown in Fig. (20), the system is constructed around a 19-inch rack which comprises all lasers, electronics, and gas connections. Its construction and functionality are described in some detail in the works by Forssén et al. [47] and Silander et al. [52].

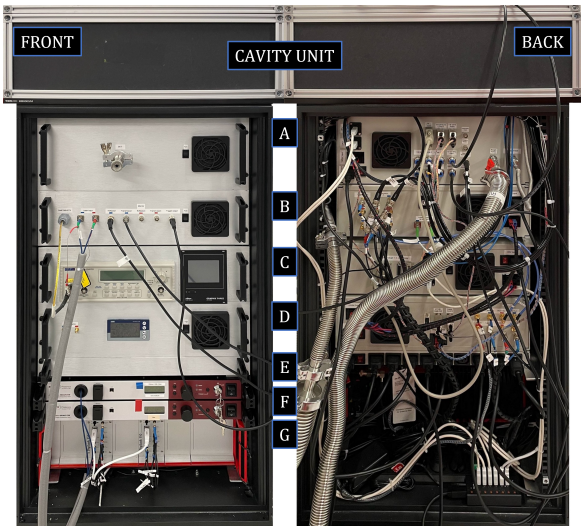

Figure 20. The TOP system seen from the front and rear. All lasers, electronics, and gas connections are placed within a 19-inch rack. On top of the rack, there is a 60 × 60 × 25 cm encapsulated box (denoted the cavity unit) that contains, as its base, an optical breadboard, on which the Invar-based DFPC is placed (in turn, encapsulated in an aluminum enclosure, denoted the "oven"). This unit also comprises four pneumatic valves that control the filling and emptying of gas in the cavity during the GAMOR-cycles and collimators, mirrors, and detectors that couple light into the cavities and measures the transmittance, respectively. The rack contains thereafter, from the top to the bottom, seven modules, denoted A-G, containing vacuum connectors, communication hub, fiber-optics, frequency counter, two fiber lasers, and locking electronics. The rack stands on four wheels that allow the system to be easily moved within the laboratory. Reproduced with permission from Ref. [47]

On top of the rack, there is a 60 × 60 × 25 cm encapsulated box (the cavity unit) that contains an optical breadboard on which the Invar-based DFPC is placed (which in turn, is encapsulated in an Al enclosure, denoted the oven). As is described above (in section 5.2.2), this unit comprises four pneumatic valves that control the filling and emptying of gas in the two cavities during the GAMOR-cycles and a number of collimators, mirrors, and detectors that couple light into the cavities and measure the reflected and the transmitted light, respectively.

The rack comprises thereafter seven modules containing vacuum connectors, communication hub, fiber-optics, a frequency counter, two fiber lasers, and locking electronics. The rack stands on four wheels that allow the system to be easily moved within the laboratory. Details of the system are given in Forssén et al. [47].

The system, whose (k=2) expanded uncertainty of the system was assessed to $[(16\ \text{mPa})^2 + (28 \times 10^{-6} P)^2]^{1/2}$, limited by the uncertainty in the temperature assessment (26 ppm), has recently been used for a circular comparison of existing primary standards at several national metrology institutes (NMIs); the measurement campaign originated from RISE and comprised PTB (Berlin), INRiM (Turin), and CNAM (Paris), before it returned to RISE [54]. One of the aims of this ring comparison was to provide information about the refractometer, its mode of operation, and its performance, including its ability to withstand ordinary commercial transportation. The result of the ring comparison, which presently is ongoing, will be reported elsewhere.

It has been established though that once the system arrived at any of the NMI laboratories it could be unpacked in a couple of hours. Although it is, in principle, directly ready for operation, it was found advantageous to let the system thermalize overnight. This is not seen as a major drawback since it gives the operator time to test and prepare the system for its task.

The experiences obtained from this ring comparison will be used for improvement of the TOP and for future realizations of transportable systems with improved performance.

8 A summary of the basic features of the GAMOR methodology

Up to hitherto, this guide has summarized the basic features of the GAMOR methodology; its principles, how it can be implemented, and its various properties. It has also provided demonstrations of its performance, in particular how it can improve on the performance of conventional (unmodulated) refractivity regarding assessment of refractivity and thereby pressure.

Irrespective of whether FPC-based refractometry is performed unmodulated or modulated, all realizations (including GAMOR-based systems) are based on the same fundamental principle; they measure the change in refractivity between two situations, with and without gas in a cavity, as a change in the frequency of laser light that is locked to a mode of the cavity. Hence, both unmodulated and modulated types of refractometry can be based on the same basic expressions, for the case with refractometry in general, given by the Eqs. (5) and (9), and, more suitable for the GAMOR methodology, given by the Eqs. (10) and (13).

While ordinary refractometry tends to emphasise that the most accurate assessments need to be performed under extraordinary well-controlled (i.e. disturbance free) conditions, the GAMOR methodology is based on a recognition of the fact that virtually all types of instrumentation are affected by various types of disturbances on some level.

Since many types of fluctuation have a $1/f^a$ dependence (where $a > 0$), the higher the frequency at which the signal is modulated and detected, the less the system is influenced by (or will pick up) fluctuations. The same is valid for drifts; the higher the frequency at which the signal is detected, the less the system is influenced by (or will pick up) a given amount of drift. Similar to various other modulated detection techniques, e.g. frequency and wavelength modulation spectrometry (FMS and WMS, respectively) and noise-immune cavity-enhanced optical-heterodyne molecular spectroscopy (NICE-OHMS)[62–65, 68, 69], the GAMOR methodology therefore strives for coding and decoding the signal at an as high frequency as possible. This is done by a modulation of the amount of gas in one of the cavities.

This is manifested through its first cornerstone, viz.

(i) the refractivity of the gas in the measurement cavity is assessed by a frequent referencing of filled measurement cavity beat frequencies to evacuated cavity beat frequencies.

To additionally reduce the influence of disturbances (primarily fluctuations and drifts) it also incorporates a second cornerstone, viz.

(ii) the evacuated measurement cavity beat frequency at the time of the assessment of the filled measurement cavity beat frequency is estimated by use of an interpolation between two evacuated measurement cavity beat frequency assessments, one performed before and one after the filled cavity assessments.

By this, the GAMOR methodology mitigates swiftly and conveniently the influence of various types of disturbances in refractometry systems, not only those from changes in length of the cavity caused by drifts in the temperature of the cavity spacer, but also several of those that have other origins (e.g., those from gas leakages and outgassing) [35, 41–45].

As described in some detail above, the GAMOR methodology has an extraordinary ability to improve on the precision of assessments of refractivity and thereby pressure. Its ability to reduce various types of fluctuations has been found to be of increasing importance the lower the addressed pressure, emphasising its role for assessments of pressures below 100 kPa.

It also provides a number of advantages that not only facilitates and improves on the assessments of refractivity and thereby pressure, it also opens up for the realization of systems based on cavity spacers in non-conventional material and transportable systems. After some initial proof-of-concept demonstrations using a cavity spacer of Zerodur [36, 41, 42], a system based on an Invar-cavity-spacer was realized [45, 46, 52]. As was mediated in section 7.2.3 above, such a cavity spacer has a number of advantages that provide several extraordinary properties that facilitate assessments of refractivity and pressure.

For example, it has been shown that it is possible to construct an Invar-based DFPC system cavity system that, when utilizing the GAMOR methodology with gas modulation periods of 100 s, is not significantly affected by thermodynamic processes that are associated with the exchange of gas (i.e., pV-work) [48, 49]. This implies that pV-work is currently not a limiting factor when the Invar-based DFPC GAMOR system is used for assessments of pressure or if it would be used as a primary pressure standard, both up to atmospheric pressure.

In addition, it has been shown that, thanks to its sub-ppm precision, it can significantly improve on the ability to assess pressure-induced cavity deformation by the use of a novel methodology that not only comprises two gases with dissimilar relativity but also performs the assessment at a series of assessments so as to additionally reduce the influence of gas leakages and outgassing [50]. It has also allowed for a methodology for accurate in-situ assessment of the penetration depth of mirrors comprising a QWS coating of type H to such an extent that the phenomenon presently does not have any significant impact on the extended uncertainty of the technique [52].

Its excellent precision has also led to an improvement of the accuracy of an instrumentation to such a level that the precision solely plays a minor (under optimal conditions, no) role in the total uncertainty budget. Up until today, it has been possible to realize a system that has demonstrated assessment of pressure with an expanded uncertainty (k=2) of $[(10\ \text{mPa})^2 + (10 \times 10^{-6}P)^2]^{1/2}$, mainly limited by the uncertainty in the molar polarizability of nitrogen (8 ppm) [52].

All this indicates that the combination of a well-characterized Invar-based DFPC system (with respect to cavity distortion and mirror penetration depth), the GAMOR methodology, and a Ga fixed-point cell can provide a basis for a self-contained system that only needs a pure gas supply and accurate frequency references to realize the Pascal. This is an important step towards the dissemination of the Pascal through fundamental principles.

9 A recipe on how to construct a GAMOR-based FPC refractometry system suitable for high precision and low uncertainty assessments

A recipe on how to implement GAMOR in a DFPC-system is as follows:

To allow for "short" gas modulation cycles:

(1) Realize a DFPC-based system with such small gas volumes that only a restricted amount of energy is brought into the cavity system with the introduction of the gas and with good thermal conductivity and no "heat islands" so that pV-work will not adversely affect the performance on the time scales utilized;

(2) Design and construct a gas handling system that automatically can modulate the amount of gas in the measurement cavity;

(3) Avoid using cavity materials and components in the gas handling system that have a large permeability to any of the gases to be used; and

(4) Create a gas evacuation system (based on the cavity volume, the tube dimensions, and the pumping effect) that allows for effective evacuation of the measurement cavity during the evacuation period.

In addition:

(5) To provide good temperature conditions, construct a temperature-stabilized environment around the cavity system, preferably with a stability in the low mK range;

(6) To avoid accumulation of gas impurities, avoid creating a system in which gas stands still — i.e., use flowing gas where possible;

(7) Utilize lasers that are tunable within a suitable wavelength range for which molecular data are provided or can be retrieved and for which there are suitable electro-optic (and, if needed, acousto-optic) components available so that the lasers can be easily tuned and sturdily locked to cavity modes;

(8) Construct a system for sturdy locking the lasers to longitudinal modes of the cavities; preferably by use of the PDH technique;

(9) Construct an optical system that allows for efficient spatial mode matching and easy optimization of the lasers to the cavity modes;

(10) To allow for autonomous assessments over any lengths of time, and to stay within the tuning range of the lasers, but also to avoid too large frequency detunings (so as to minimize the influence of the group delay dispersion, GDD), provide means to automatically and rapidly (preferably within a second) relock the lasers (e.g., by detecting and using also the transmitted light);

(11) Assess, with adequate accuracy, the empty cavity frequencies of the two lasers, i.e., ν_{0m} and ν_{0r};

(12) Design and utilize a method to assess the values of the numbers of the modes at which the empty cavity frequencies are assessed, i.e., m_{0m} and m_{0r}, preferably with no uncertainty;

(13) Design and utilize a method to automatically keep track of the numbers of the modes addressed in terms of deviations from m_{0m} and m_{0r}, i.e., the $\Delta m_m(t)$ and $\Delta m_r(t)$ entities;

(14) Provide means to assess, in a repeated manner, the beat frequency between the two lasers, i.e., the $f(t)$;

(15) Provide means to assess the temperature of the gas, $T(t)$, preferably by assessing the temperature of the cavity spacer repeatedly, with a stability in the low or sub-mK range;

(16) Create a data acquisition system that can assess all repeatedly assessed input parameters, primarily the $f(t)$, $\Delta m_m(t)$, $\Delta m_r(t)$, and $T(t)$, in a synchronous manner with clearly defined time stamps;

(17) Estimate the value of the Gouy phase parameter, Θ_G;

(18) Characterize (or estimate) the penetration depths of the mirrors in terms of the γ_c entity (or, when the mirrors are not used around their center frequency, γ_s'), possibly using the methodology developed by Silander et al. [51];

(19) Assess, from the ν_{0m}, Θ_G, m_{0m}, and γ_c (or γ_s') entities, the ν_{0m}' entity for the measurement cavity;

(20) Assess the ν_{0r}' for the reference cavity from the corresponding entities for that cavity;

(21) Provide means to automatically assess, by the use of Eq. (10) and the $f(t)$, $\Delta m_m(t)$, $\Delta m_r(t)$, m_{0m}, m_{0r}, ν_{0m}', and ν_{0r}' entities, the unwrapped beat frequency, i.e., the $f_{UW}(t)$ entity;

(22) To be able to implement cornerstone 2, create, based on pair-wise assessments of the "baseline" [i.e. the unwrapped beat frequency entity when both cavities are evacuated, i.e., $f_{UW}^{(0)}(t_{k+1})$ and $f_{UW}^{(0)}(t_k)$], by interpolation, according to Eq. (11), an estimate of the empty cavity beat frequency for all time instants during a gas modulation cycle, $\tilde{f}_{UW}^{(0)}(t)$;

(23) To create the $\Delta f_{UW}(t)$ entity, relate, at each time instant, according to Eq. (12), the unwrapped beat frequency measured with gas in the measurement cavity, $f_{UW}^{(g)}(t)$, to the interpolated "baseline", $\tilde{f}_{UW}^{(0)}(t)$;

(24) Characterize the system with respect to its refractivity normalized pressure induced deformation, ε', (for the case when the relative elongation is considered to be linear with pressure and when nitrogen is assessed, to ε_0') possibly using the methodology developed by Zakrisson et al. [50];

(25) Assess, from the $\Delta f_{UW}(t)$, ν_{0m}', $\Delta m_m(t)$, m_{0m}, Θ_G, and ε' (or ε_0') entities, the refractivity, $(n-1)(t)$, by use of Eq. (13);[25]

(26) To certify that the assessments are not influenced by thermodynamic effects, assess the lower limit of the gas modulation period for which the assessments are not noticeably influenced by any pV-work, and use modulation times equal to or longer than this;

(27) Assess the molar density and pressure by use of the Lorentz-Lorenz equation and an appropriate equation of state. For the case of nitrogen, and for pressures up to 10^5 Pa, use the Eqs. (14) and (15) with appropriate molecular parameter values from the literature;

(28) To reduce the influence of white noise, assess, by a series of measurements, the optimum intra-cycle averaging time for assessment of the beat frequency under both filled and empty measurement cavity conditions; and

(29) To optimize the system, assess the optimum modulation and detection conditions for the system (e.g., the number of modulation cycled over which the data are averaged) by analyzing the assessed pressure by an Allan variance analysis.

By this, refractivity, molar density, and pressure, can be assessed or realized by DFPC-based refractometry with higher precision than if unmodulated refractometry would be used, and, if precision has been a sizeable part of the uncertainty, also an improved uncertainty.

[25] For the case when not both the conditions that the relative elongation is linear with pressure and nitrogen is addressed hold, Eq. (13) should to be exchanged to a corresponding one based on Eq. (5).

References

[1] C. R. Tilford. Three and a half centuries later - the modern art of liquid-column manometry. *Metrologia*, 30(6):545–552, jan 1994. doi: 10.1088/0026-1394/30/6/001.

[2] S. Semenoja and M. Rantanen. Comparisons to establish a force-balanced piston gauge and a spinning rotor gauge as the new measurement standards of mikes. *Vacuum*, 73:269–274, 03 2004. doi: 10.1016/j.vacuum.2003.12.007.

[3] J. Hendricks and D. Olson. 1–15,000Pa Absolute mode comparisons between the NIST ultrasonic interferometer manometers and non-rotating force-balanced piston gauges. *Measurement*, 43(5):664–674, jun 2010. ISSN 02632241. doi: 10.1016/j.measurement.2009.12.031.

[4] J. W. Schmidt, K. Jain, A. P. Miiller, W. J. Bowers, and D. A. Olson. Primary pressure standards based on dimensionally characterized piston/cylinder assemblies. *Metrologia*, 43(1):53–59, nov 2005. doi: 10.1088/0026-1394/43/1/008.

[5] J. Ricker, J. Hendricks, T. Bock, K. Dominik, T. Kobata, J. Torres, and I. Sadkovskaya. Final report on the key comparison CCM.p-k4.2012 in absolute pressure from 1 pa to 10 kPa. *Metrologia*, 54(1A):07002–07002, dec 2016. doi: 10.1088/0026-1394/54/1a/07002.

[6] M. Stock, R. Davis, E. de Mirandés, and M. J. T. Milton. The revision of the SI—the result of three decades of progress

in metrology. *Metrologia*, 56(4):022001, aug 2019. ISSN 0026-1394. doi: 10.1088/1681-7575/ab0013.

[7] M. Stock, R. Davis, E. de Mirandés, and M. J. T. Milton. Corrigendum: The revision of the SI—the result of three decades of progress in metrology. *Metrologia*, 56(4):49502, aug 2019. ISSN 0026-1394. doi: 10.1088/1681-7575/ab28a8.

[8] M. Puchalski, K. Szalewicz, M. Lesiuk, and B. Jeziorski. Qed calculation of the dipole polarizability of helium atom. *Phys. Rev. A*, 101:022505, Feb 2020. doi: 10.1103/PhysRevA.101.022505.

[9] K. Jousten, J. Hendricks, D. Barker, K. Douglas, S. Eckel, P. Egan, J. Fedchak, J. Flügge, C. Gaiser, D. Olson, J. Ricker, T. Rubin, W. Sabuga, J. Scherschligt, R. Schödel, U. Sterr, J. Stone, and G. Strouse. Perspectives for a new realization of the pascal by optical methods. *Metrologia*, 54(6):S146—-S161, 2017. ISSN 16817575. doi: 10.1088/1681-7575/aa8a4d.

[10] A. D. Buckingham and C. Graham. The Density Dependence of the Refractivity of Gases. *Proceedings of the Royal Society A: Mathematical, Physical and Engineering Sciences*, 337(1609): 275–291, mar 1974. ISSN 1364-5021. doi: 10.1098/rspa.1974.0049.

[11] M. Jaeschke, H. M. Hinze, H. J. Achtermann, and G. Magnus. PVT data from burnett and refractive index measurements for the nitrogen—hydrogen system from 270 to 353 K and pressures to 30 MPa. *Fluid Phase Equilibria*, 62(1-2):115–139, jan 1991. ISSN 03783812. doi: 10.1016/0378-3812(91)87010-7.

[12] H. J. Achtermann, G. Magnus, and T. K. Bose. Refractivity virial coefficients of gaseous CH_4, C_2H_4, C_2H_6, CO_2, SF_6, H_2, N_2, He, and Ar. *J. Chem. Phys.*, 94(8):5669–5684, apr 1991. ISSN 0021-9606. doi: 10.1063/1.460478.

[13] H. Fang, A. Picard, and P. Juncar. A heterodyne refractometer for air index of refraction and air density measurements. *Review of Scientific Instruments*, 73(4):1934–1938, apr 2002. ISSN 0034-6748. doi: 10.1063/1.1459091.

[14] L. R. Pendrill. Refractometry and gas density. *Metrologia*, 41(2):S40–S51, apr 2004. ISSN 0026-1394. doi: 10.1088/0026-1394/41/2/S04.

[15] J. A. Stone and A. Stejskal. Using helium as a standard of refractive index: Correcting errors in a gas refractometer. *Metrologia*, 41 (3):189–197, 2004. ISSN 00261394. doi: 10.1088/0026-1394/41/3/012.

[16] P. F. Egan and J. A. Stone. Absolute refractometry of dry gas to ±3 parts in 10^9. *Appl. Opt.*, 50:3076, 2011. doi: 10.1364/AO.50.003076.

[17] P. Egan, J. Stone, J. Hendricks, J. Ricker, G. Scace, and G Strouse. Performance of a dual fabry-perot cavity refractometer. *Opt. Lett.*, 40(17):3945–3948, Sep 2015. doi: 10.1364/OL.40.003945.

[18] M Andersson, L Eliasson, and L R Pendrill. Compressible Fabry-Perot refractometer. *Applied Optics*, 26(22):4835, nov 1987. ISSN 0003-6935. doi: 10.1364/AO.26.004835.

[19] I. Silander, M. Zelan, O. Axner, F. Arrhén, L. Pendrill, and A. Foltynowicz. Optical measurement of the gas number density in a Fabry–Perot cavity. *Measurement Science and Technology*, 24(10):105207, oct 2013. ISSN 0957-0233. doi: 10.1088/0957-0233/24/10/105207.

[20] D. Mari, M. Bergoglio, M. Pisani, and M. Zucco. Dynamic vacuum measurement by an optical interferometric technique. *Meas. Sci. Technol.*, 25:125303, 2014. doi: 10.1088/0957-0233/25/12/125303.

[21] Y. Takei, K. Arai, H. Yoshida, Y. Bitou, S. Telada, and T. Kobata. Development of an optical pressure measurement system using an external cavity diode laser with a wide tunable frequency range. *Measurement: Journal of the International Measurement Confederation*, 151:107090, 2020. ISSN 02632241. doi: 10.1016/j.measurement.2019.107090.

[22] Z. Silvestri, D. Bentouati, P. Otal, and J. P. Wallerand. Towards an improved helium-based refractometer for pressure measurements. *Acta IMEKO*, 9:303, 2020. doi: 10.21014/ACTA_IMEKO.V9I5.989.

[23] F. Riehle, P. Gill, F. Arias, and L. Robertsson. The CIPM list of recommended frequency standard values: guidelines and procedures. *Metrologia*, 55(2):188–200, feb 2018. doi: 10.1088/1681-7575/aaa302.

[24] S. Häfner, S. Falke, C. Grebing, S. Vogt, T. Legero, M. Merimaa, C. Lisdat, and U. Sterr. 8×10^{-17} fractional laser frequency instability with a long room-temperature cavity. *Opt. Lett.*, 40(9):2112–2115, May 2015. doi: 10.1364/OL.40.002112.

[25] Y. Y. Jiang, A. D. Ludlow, N. D. Lemke, R. W. Fox, J. A. Sherman, L. S. Ma, and C. W. Oates. Making optical atomic clocks more stable with 10-16-level laser stabilization. *Nature Photonics*, 5(9):1749–4893, 2011. doi: 10.1038/nphoton.2010.313.

[26] M. L. Eickhoff and J. L. Hall. Real-time precision refractometry: new approaches. *Appl. Opt.*, 36(6):1223–1234, Feb 1997. doi: 10.1364/AO.36.001223.

[27] N. Khélifa, H. Fang, J. Xu, P. Juncar, and M. Himbert. Refractometer for tracking changes in the refractive index of air near 780 nm. *Appl. Opt.*, 37(1):156–161, Jan 1998. doi: 10.1364/AO.37.000156.

[28] R. W. Fox, B. R. Washburn, N. R. Newbury, and L. Hollberg. Wavelength references for interferometry in air. *Appl. Opt.*, 44(36):7793–7801, Dec 2005. doi: 10.1364/AO.44.007793.

[29] G. Z. Xiao, A. Adnet, Z. Zhang, F. G. Sun, and C. P. Grover. Monitoring changes in the refractive index of gases by means of a fiber optic fabry-perot interferometer sensor. *Sensors and Actuators A: Physical*, 118 (2):177–182, 2005. ISSN 0924-4247. doi: 10.1016/j.sna.2004.08.029.

[30] P. Egan, J. Stone, J. Ricker, and J. Hendricks. Comparison measurements of low-pressure between a laser refractometer and ultrasonic manometer. *Review of Scientific Instruments*, 87(5):053113, 2016. ISSN 10897623. doi: 10.1063/1.4949504.

[31] Y. Yang and T. Rubin. Simulation of pressure induced length change of an optical cavity used for optical pressure standard. *Journal of Physics: Conference Series*, 1065: 162003, aug 2018. doi: 10.1088/1742-6596/1065/16/162003.

[32] R. W. Fox. Temperature analysis of low-expansion fabry-perot cavities. *Opt. Express*, 17(17):15023–15031, Aug 2009. doi: 10.1364/OE.17.015023.

[33] M. Zelan, I. Silander, T. Hausmaninger, and O. Axner. Fast Switching Dual Fabry-Perot-Cavity-based Optical Refractometry for Assessment of Gas Refractivity and Density - Estimates of Its Precision, Accuracy, and Temperature Dependence. *arXiv: 1704.01185v2*, apr 2017.

[34] H. Fang and P. Juncar. A new simple compact refractometer applied to measurements of air density fluctuations. *Review of Scientific Instruments*, 70(7):3160–3166, jul 1999. ISSN 00346748. doi: 10.1063/1.1149880.

[35] O. Axner, I. Silander, T. Hausmaninger, and M. Zelan. Drift-free fabry-perot-cavity-based optical refractometry—accurate expressions for assessments of gas refractivity and density. e-print arXiv:1704.01187v2, 2017.

[36] I. Silander, T. Hausmaninger, M. Bradley, M. Zelan, and O. Axner. Fast Switching Dual Fabry-Perot Cavity Optical Refractometry - Methodologies for Accurate Assessment of Gas Density. *arXiv:1704.01186v2*, apr 2017.

[37] J. H. Hendricks, G. F. Strouse, J. E. Ricker, D. A. Olson, G. E. Scace, J. A. Stone, and P. F. Egan. Photonic article, process for making and using same, January 2015.

[38] E. Hedlund and L. R. Pendrill. Improved determination of the gas flow rate for UHV and leak metrology with laser refractometry. *Measurement Science and Technology*, 17(10): 2767–2772, oct 2006. ISSN 0957-0233. doi: 10.1088/0957-0233/17/10/031.

[39] E Hedlund and L R Pendrill. Addendum to 'Improved determination of the gas flow rate for UHV and leak metrology with laser refractometry'. *Measurement Science and Technology*, 18

(11):3661–3663, nov 2007. ISSN 0957-0233. doi: 10.1088/0957-0233/18/11/052.

[40] A. Picard and H. Fang. Three methods of determining the density of moist air during mass comparisons. *Metrologia*, 39(1):31–40, feb 2002. doi: 10.1088/0026-1394/39/1/5.

[41] I. Silander, T. Hausmaninger, M. Zelan, and O. Axner. Gas modulation refractometry for high-precision assessment of pressure under non-temperature-stabilized conditions. *J. Vac. Sci. Technol. A*, 36:03E105, 2018. doi: 10.1116/1.5022244.

[42] I. Silander, T. Hausmaninger, C. Forssén, M. Zelan, and O. Axner. Gas equilibration gas modulation refractometry for assessment of pressure with sub-ppm precision. *Journal of Vacuum Science & Technology B*, 37(4):042901, 2019. doi: 10.1116/1.5090860.

[43] O. Axner, I. Silander, C. Forssén, J. Zakrisson, and M. Zelan. Ability of gas modulation to reduce the pickup of fluctuations in refractometry. *Journal of the Optical Society of America B*, 37(7):1956–1965, 2020. ISSN 0740-3224. doi: 10.1364/josab.387902.

[44] O. Axner, C. Forssén, I. Silander, J. Zakrisson, and M. Zelan. Ability of gas modulation to reduce the pickup of drifts in refractometry. *J. Opt. Soc. Am. B*, 38(8):2419–2436, Aug 2021. doi: 10.1364/JOSAB.420982.

[45] I. Silander, C. Forssén, J. Zakrisson, M. Zelan, and O. Axner. Invar-based refractometer for pressure assessments. *Optics Letters*, 45 (9):2652–2655, 2020. ISSN 0146-9592. doi: 10.1364/ol.391708.

[46] I. Silander, C. Forssén, J. Zakrisson, M. Zelan, and O. Axner. An invar-based Fabry-Perot cavity refractometer with a gallium fixed-point cell for assessment of pressure. *Acta IMEKO*, 9(5):293–298, 2020. ISSN 2221870X. doi: 10.21014/ACTA_IMEKO.V9I5.987.

[47] C. Forssén, I. Silander, J. Zakrisson, O. Axner, and M. Zelan. The short-term performances of two independent gas modulated refractometers for pressure assessments. *Sensors*, 21(18), 2021. ISSN 1424-8220. doi: 10.3390/s21186272.

[48] T. Rubin, I. Silander, M. Bernien, C. Forssen, J. Zakrisson, M. Hao, P. Kussicke, .and Asbahr, M. Zelan, and O. Axner. Thermodynamic effects in a gas modulated Invar-based dual Fabry-Perot cavity refractometer. *Metrologia*, 59:035003, 2022. doi: 10.1088/1681-7575/ac5ef9.

[49] T. Rubin, I. Silander, J. Zakrisson, M. Hao, C. Forssén, P. Asbahr, M. Bernien, A. Kussicke, K. Liu, M. Zelan, and O. Axner. Thermodynamic effects in a gas modulated Invar-based dual Fabry-Pérot cavity refractometer addressing 100 kPa of nitrogen. *Acta IMEKO, in press*, x(x):xxx–xxx, 2022. ISSN xxx. doi: xxx.

[50] J. Zakrisson, I. Silander, C. Forssén, M. Zelan, and O. Axner. Procedure for robust assessment of cavity deformation in Fabry–Pérot based refractometers. *J. Vac. Sci. Technol. B*, 38:054202, 2020. doi: 10.1116/6.0000375.

[51] I. Silander, J. Zakrisson, V. Silvia de Oliveira, C. Forssén, A. Foltynowicz, M. Zelan, and O. Axner. In situ determination of the penetration depth of mirrors in Fabry-Perot refractometers and its influence on assessment of refractivity and pressure. *Optics Express*, 30(14): 25891–25906, 2022. ISSN 1094-4087. doi: 10.1364/OE.463285.

[52] I. Silander, C. Forssén, J. Zakrisson, M. Zelan, and O. Axner. Optical realization of the Pascal—Characterization of two gas modulated refractometers. *J. Vac. Sci. Technol. B*, 39: 044201, 2021. doi: 10.1116/6.0001042.

[53] C. Forssén, I. Silander, D. Szabo, G. Jönsson, M. Bjerling, T. Hausmaninger, O. Axner, and M. Zelan. A transportable refractometer for assessment of pressure in the kPa range with ppm level precision. *Acta IMEKO*, 9 (5):287–292, 2020. ISSN 2221870X. doi: 10.21014/ACTA_IMEKO.V9I5.986.

[54] C. Forssén, I. Silander, J. Zakrisson, E Amer, D Szabo, T. Bock, A Kussicke, T. Rubin, D. Mari, S. Pasqualin, Z. Silvestri, D. Bentouari, O. Axner, and M. Zelan. Circular comparison of conventional pressure standards using a transportable optical refractometer. *Acta IMEKO, in press*, x(x):xxx–xxx, 2022. ISSN xxx. doi: xxx.

[55] M. Zelan, I. Silander, C. Forssén, J. Zakrisson, and O. Axner. Recent advances in Fabry-Perot-based refractometry utilizing gas modulation for assessment of pressure. *Acta IMEKO*, 9 (5):299–304, 2020. ISSN 2221870X. doi: 10.21014/ACTA_IMEKO.V9I5.988.

[56] O. Axner, I. Silander, C. Forssén, J. Zakrisson, and Zelan. M. Assessment of gas molar density by gas modulation refractometry: A review of its basic operating principles and extraordinary performance. *Spectrochim. Acta B*, 179:106121, 2021. doi: 10.1016/j.sab.2021.106121.

[57] C. Forssén, I. Silander, J. Zakrisson, M. Zelan, and O. Axner. An Optical Pascal in Sweden. *Sensors*, 24:033002, 2022. doi: 10.1088/2040-8986/ac4ea2.

[58] T. Rubin, I. Silander, C. Forssén, J. Zakrisson, E Amer, D. Szabo, T. Bock, A. Kussicke, C. Günz, D. Mari, R. M. Gavioso, M. Pisani, S. Pasqualin, D. Madonna Ripa, Z. Silvestri, P. Gambette, D. Bentouari, G. Garberoglio, M. Lesiuk, M. Przybytek, B. Jeziorski, J. Setina, M. Zelan, and O. Axner. 'Quantum-based realizations of the pascal' status and progress of the empir-project: Quantumpascal. *Acta IMEKO, in press*, x(x):xxx–xxx, 2022. ISSN xxx. doi: xxx.

[59] C. Koks and M. P. van Exter. Microcavity resonance condition, quality factor, and mode volume are determined by different penetration depths. *Opt. Express*, 29:6879, 2021. doi: 10.1364/OE.412346.

[60] J. Zakrisson, I. Silander, C. Forssén, M. Zelan, T. Rubin, A. Kussicke, Z. Silvestri, and O. Axner. Pressure-induced cavity deformation in fabry-pérot refractometry - characterization and recommendations. *Report on the A1.1.4 activity in the EMPIR project 18SIB04, "QuantumPascal"*, 2022.

[61] P. Egan, J. Stone, J. Scherschligt, and Allan H. Harvey. Measured relationship between thermodynamic pressure and refractivity for six candidate gases in laser barometry. *Journal of Vacuum Science & Technology A*, 37(3):031603, 2019. ISSN 0734-2101. doi: 10.1116/1.5092185.

[62] J. A. Silver. Frequency-modulation spectroscopy for trace species detection: theory and comparison among experimental methods. *Appl. Opt.*, 31:707–717, 1992. doi: 10.1364/AO.31.000707.

[63] D. S. Bomse, A. C. Stanton, and J. A. Silver. Frequency modulation and wavelength modulation spectroscopies: comparison of experimental methods using a lead-salt diode laser. *Appl. Opt.*, 31:718–731, 1992. doi: 10.1364/AO.31.000718.

[64] J. M. Supplee, E. A. Whittaker, and T. Lenth. Theoretical description of frequency modulation and wavelength modulation spectroscopy. *Appl. Opt.*, 33:6294–6302, 1994. doi: 10.1364/AO.33.006294.

[65] P. Kluczynski and O. Axner. Theoretical description based on fourier analysis of wavelength-modulation spectrometry in terms of analytical and background signals. *Appl. Opt.*, 38(27):5803–5815, Sep 1999. doi: 10.1364/AO.38.005803.

[66] R. W. P. Drever, J. L. Hall, F. V. Kowalski, J. Hough, G. M. Ford, A. J. Munley, and H. Ward. Laser phase and frequency stabilization using an optical resonator. *Applied Physics B Photophysics and Laser Chemistry*, 31 (2):97–105, jun 1983. ISSN 0721-7269. doi: 10.1007/BF00702605.

[67] T. Rubin, A. Kussicke, M. G. Gonzalez, Z. Silvestri, M. Zelan, C. Forssén, I. Silander, J. Zakrisson, and O. Axner. Development of methods for control and assessment of the temperature of the gas in fabry-pérot cavities. *Report on the A1.2.3 activity in the EMPIR project 18SIB04, "QuantumPascal"*, 2022.

[68] A. Foltynowicz, F. M. Schmidt, W. Ma, and O. Axner. Noise-immune cavity-enhanced optical heterodyne molecular spectroscopy: Current status and future potential. *Appl. Phys. B*, 92:313–326, Sep 2008. doi: 10.1007/s00340-008-3126-z.

[69] G. Zhao, T. Hausmaninger, W. Ma, and O. Axner. Shot-noise-limited doppler-broadened noise-immune cavity-enhanced optical heterodyne molecular spectrometry. *Opt. Lett.*, 43(4):715–718, Feb 2018. doi: 10.1364/OL.43.000715.

Appendix

A. Derivation of expressions for the refractivity in FPC-based refractometry in the presence of mirrors comprising a quarter-wave stack (QWS) coating of type H and the Gouy phase

Following [59], the round-trip resonance condition of the m^{th} TEM_{00} mode of a FP cavity with DBR mirrors can be written as

$$2k_{in}(L_0+\delta L)+\phi_1+\phi_2-2\Theta_G=2\pi m, \tag{A.1}$$

where k_{in} is the wave vector of the light in the cavity, L_0 the distance between the front facets of the two DBRs coatings of the mirrors, δL the pressure induced cavity deformation, ϕ_1 and ϕ_2 the reflection phases of the two DBR equipped mirrors, Θ_G the (single pass) Gouy phase, and m an integer, representing the number of the longitudinal mode the laser addresses.

For the case with two identical mirrors, as is assumed here, it is convenient to assume that $\phi_1=\phi_2=\phi$.

1. For working ranges centred on the mirror center frequency

Assuming that the laser frequency is close to the design frequency, ν_c, where the non-linear contributions to the phase can be neglected, it is possible to express ϕ as $(\partial\phi/\partial\omega)(\omega-\omega_c)$. It is customary to define $(\partial\phi/\partial\omega)$ as the delay an optical pulse experiences upon reflection from a DBR when its spectrum fits well within the stop-band of the coating, commonly referred to as the group delay and generally denoted $\tau_c(n)$, where the subscript $_c$ indicates that it refers to the mirror center frequency and n is the index of refraction of the gas in front of the mirror (which, in this case, is in the cavity). This implies that it is possible to express ϕ in terms of the natural frequencies, ν and ν_c, as $2\pi\tau(n)(\nu-\nu_c)$.

Since k_{in} in general is given by $n(\omega/c)$, this implies that Eq. (A.1) can be expressed as

$$2n(L_0+\delta L)\nu+2c\tau_c(n)(\nu-\nu_c)=c\left(m+\frac{\Theta_G}{\pi}\right). \tag{A.2}$$

As is shown by Silander et al. [51], solving this for ν [assuming Θ_G and $\tau_c(n)$ to be independent of the frequency of the light, which is a most reasonable assumption for the cases when the laser frequency makes recurring mode jumps whereby the maximum shift in frequency is the free-spectral-range, FSR, of the cavity] gives

$$\nu=\frac{c\left[m+\frac{\Theta_G}{\pi}+2\tau_c(n)\nu_c\right]}{2\left[n(L_0+\delta L)+c\tau_c(n)\right]}=\frac{cm\left[1+\frac{\Theta_G}{\pi m}+\frac{n\gamma_c(n)}{m}\right]}{2n\left[L_0+\delta L+2L_{\tau,c}(n)\right]}, \tag{A.3}$$

where we in the last step have introduced $\gamma_c(n)$, formally defined by $\frac{2\tau_c(n)\nu_c}{n}$, and $L_{\tau,c}(n)$, given by $\frac{c\tau_c(n)}{2n}$, where the latter represents the frequency penetration depth of a single mirror [$2L_\tau(n)$ thus represents the elongation of the length of the cavity experienced during scans due to the penetration of light into the mirror coatings].

For a mirror coating of type H, $\tau_c(n)$ is given by $\frac{n}{n_H-n_L}\frac{1}{2\nu_c}$, where n_H and n_L are the indices of refraction for the coating layers with highest and lowest index of refraction, respectively [59]. This implies that, for this type of coating, both $\gamma_c(n)$ and $L_{\tau,c}(n)$ are purely material-dependent, but index-of-refraction-independent, parameters, that therefore henceforth can be written as γ_c and $L_{\tau,c}$, given by $\frac{1}{n_H-n_L}$ and $\frac{c\gamma_c}{4\nu_c}$, respectively.

This implies that the frequency of the mode of the cavity the laser addresses in the absence of gas (i.e. the m_0^{th} mode), ν_0, can be written as

$$\nu_0=\frac{cm_0\left(1+\frac{\Theta_G}{\pi m_0}+\frac{\gamma_c}{m_0}\right)}{2\left(L_0+2L_{\tau,c}\right)}. \tag{A.4}$$

Hence, when gas is filled into the cavity, the laser will shift its frequency an amount, $\Delta\nu$, defined as $\nu_0-\nu$, given by

$$\Delta\nu = \nu_0 - \frac{cm\left(1+\frac{\Theta_G}{\pi m}+\frac{n\gamma_c}{m}\right)}{2n\left(L_0+\delta L+2L_{\tau,c}\right)}. \tag{A.5}$$

Making use of the expression for the frequency of the mode of the cavity the laser addresses in the absence of gas, i.e. Eq. (A.4), it is possible, by use of Eq. (A.5), to write an expression for the relative shift in frequency of the laser light when gas is filled into the cavity, i.e. $\frac{\Delta\nu}{\nu_0}$, as

$$\frac{\Delta\nu}{\nu_0} = 1-\frac{1}{n}\frac{m\left(1+\frac{\Theta_G}{\pi m}+\frac{n\gamma_c}{m}\right)}{m_0\left(1+\frac{\Theta_G}{\pi m_0}+\frac{n\gamma_c}{m_0}\right)}\frac{1}{1+\delta L/L'}, \tag{A.6}$$

where we have introduced the notation L' for the effective length of the empty cavity comprising coated mirrors experienced during a scan, given by $L_0+2L_{\tau,c}$.

Solving this expression for $n-1$ gives

$$n-1 = \frac{\frac{\Delta\nu}{\nu_0}\left(1+\frac{\Theta_G}{\pi m_0}+\frac{\gamma_c}{m_0}\right)+\frac{\Delta m}{m_0}-\frac{\delta L}{L'}(1-\frac{\Delta\nu}{\nu_0})\left(1+\frac{\Theta_G}{\pi m_0}+\frac{\gamma_c}{m_0}\right)}{(1-\frac{\Delta\nu}{\nu_0})(1+\frac{\delta L}{L'})\left(1+\frac{\Theta_G}{\pi m_0}+\frac{\gamma_c}{m_0}\right)-\frac{\gamma_c}{m_0}}. \tag{A.7}$$

where Δm is the shift of the mode number, given by $m-m_0$.

Noting that $\frac{\delta L}{L'}$, to first order, is linear with pressure (and thereby refractivity), it is convenient to introduce ε' as the refractivity-normalized relative elongation of the FSR of the cavity due to the presence of the gas, defined as $\frac{\delta L}{L'}\frac{1}{n-1}$. By doing this, it can be noted that the last term in the numerator, which is proportional to $\frac{\delta L}{L'}$, has a linear dependence on refractivity, i.e. it is proportional to $(n-1)$. Merging this term with the left hand side of the expression implies that it is possible to derive an expression for the refractivity that is given by

$$n-1 = \frac{\frac{\Delta\nu}{\nu_0}(1+\frac{\Theta_G}{\pi m_0}+\frac{\gamma_c}{m_0})+\frac{\Delta m}{m_0}}{1-\frac{\Delta\nu}{\nu_0}(1+\frac{\Theta_G}{\pi m_0}+\frac{\gamma_c}{m_0})+\frac{\Theta_G}{\pi m_0}+n\varepsilon'(1+\xi_c)}, \tag{A.8}$$

where we have introduced the entity ξ_c, defined as $\xi_c = (1+\frac{\Theta_G}{\pi m_0}+\frac{\gamma_c}{m_0})(1-\frac{\Delta\nu}{\nu_0})-1$. It is worth to note that Eq. (A.8) is, for the case with mirror coatings comprising a QWS of type H, mathematically identical to Eq. (A.1).

Since, for all practical purposes, $\xi_c \approx \frac{\Theta_G}{\pi m_0}+\frac{\gamma_c}{m_0}-\frac{\Delta\nu}{\nu_0} \approx \left(\frac{\Theta_G}{\pi}+\gamma_c-1\right)\frac{\Delta\nu}{\nu_0}$, for standard types of cavities (with a length of some tens of cm and with mirrors with curvatures of 0.5 m, for which $\frac{\Theta_G}{\pi}<1$ and $\frac{\Delta\nu}{\nu_0}$ maximally is in the mid 10^{-6} range, and for a typical QWS for which $0.5<\gamma_c<2$), $n\varepsilon'\xi_c$ is maximally in the 10^{-9} to the low 10^{-8} range, thus significantly smaller than unity. This implies that it is possible to neglect the influence of ξ_c in the expression for the refractivity above and write it as

$$n-1 = \frac{\frac{\Delta\nu}{\nu_0}(1+\frac{\Theta_G}{\pi m_0}+\frac{\gamma_c}{m_0})+\frac{\Delta m}{m_0}}{1-\frac{\Delta\nu}{\nu_0}(1+\frac{\Theta_G}{\pi m_0}+\frac{\gamma_c}{m_0})+\frac{\Theta_G}{\pi m_0}+n\varepsilon'}. \tag{A.9}$$

Moreover, as is shown by Eq. (SM-15) in the supplementary material to Zakrisson et al. [50], under the condition that $\frac{\delta L}{L_0'}$ can be written as κP, and by using an equation of state and the Lorentz-Lorenz expression, it is possible to conclude that ε' is an entity that has a weak dependence on refractivity (for low pressures it acts as a constant and for higher it is weakly dependent on the refractivity) that can be written as $\varepsilon_0'[1+\xi_2(T)(n-1)]$, where ε_0' is given by $\kappa RT\frac{2}{3A_R}$ and $\xi_2(T)$ is given by a combination of density and refractivity virial coefficients.

This implies that Eq. (A.9) can be expressed as

$$n-1=\frac{\frac{\Delta\nu}{\nu_0}(1+\frac{\Theta_G}{\pi m_0}+\frac{\gamma_c}{m_0})+\frac{\Delta m}{m_0}}{1-\frac{\Delta\nu}{\nu_0}(1+\frac{\Theta_G}{\pi m_0}+\frac{\gamma_c}{m_0})+\frac{\Theta_G}{\pi m_0}+\varepsilon_0'+(n-1)\varepsilon_0'[1+\xi_2(T)]}. \tag{A.10}$$

Although this is a recursive equation in $n-1$, the recursivity is very weak for most gas species. For nitrogen, for example, it has been estimated by Zakrisson et al. that, at a temperature of 296.15 K, $\xi_2(T)$ takes a value of -1.00(4) [50]. This implies that the $\xi_2(T)$ term fully cancels the unity term in the non-linear $(n-1)\varepsilon_0'[1+\xi_2(T)]$ term in the denominator. For temperatures close to, but not exactly at, this, $\xi_2(T)$ differs solely slightly from -1.00(4). Since, for the Invar-based cavity system used in this work [45], for which ε_0' has been found to be ca. 2×10^{-3}, and for the case when nitrogen is addressed, $(n-1)\varepsilon_0'$ is solely 0.54×10^{-6} at 100 kPa, this implies that the $(n-1)\varepsilon_0'[1+\xi_2(T)]$ term can, also for a range of temperatures around 296 K, and as long as pressures of nitrogen up to 100 kPa are addressed, safely be neglected. In this case, Eq. (A.10) can be written more succinctly as

$$n-1=\frac{\frac{\Delta\nu}{\nu_0}(1+\frac{\Theta_G}{\pi m_0}+\frac{\gamma_c}{m_0})+\frac{\Delta m}{m_0}}{1-\frac{\Delta\nu}{\nu_0}(1+\frac{\Theta_G}{\pi m_0}+\frac{\gamma_c}{m_0})+\frac{\Theta_G}{\pi m_0}+\varepsilon_0'}. \tag{A.11}$$

Since ε_0' is a constant (index of refraction independent) entity, this implies that, by use of the refraction-normalized relative deformation concept (i.e. ε' and ε_0' entities), $n-1$ can, when nitrogen is addressed, be expressed in terms of a recursive-free expression. This facilitates significantly the assessment of refractivity from measurement data.

It is worth to note that the step that brings Eq. (A.10) into Eq. (A.11) is not appropriate when He is addressed, since $\xi_2(T)$ for He takes a value of -15.208(1) (at 296.15 K). In this case, Eq. (A.10) needs to be used instead of Eq. (A.11).

2. For working ranges not centred on the mirror center frequency

As is shown in Silander et al. [51], when the mirrors are not used around their mirror center frequency, the reflection phase should preferably be expressed in terms of a Taylor series expended around the center frequency of the working range, denoted ν_s. In this case, the cavity mode frequencies and refractivity given above, i.e. the Eqs. (A.3), (A.4), (A.9) - (A.11), can be used as long as the $L_{\tau,c}$ and γ_c are replaced by $L_{\tau,s}$ and γ_s', which are given by $\frac{c\tau_s(n)}{2n}$ and $\gamma_s\left(1+\frac{1+\chi_0}{1+\chi_1}\frac{\Delta\nu_{cs}}{\nu_s}\right)$, where, in turn, $\tau_s(n)$ is the GD at the center frequency of the light, γ_s is given by $\frac{2\tau_s(n)\nu_s}{n}$, $\Delta\nu_{cs}$ represents the frequency difference between the mirror center frequency and the center of the working range, i.e. $\nu_c-\nu_s$, while χ_0 and χ_1 represent the relative contributions of the group delay dispersion (GDD) and the next higher order dispersion term in the Taylor expansion of the phase shift of the reflection of light at the front facets of the mirrors respectively, given by Table 1 in the Supplementary material in Ref. [51].

3. Comparison with previously used nomenclature

Although Eq. (A.11) is fully adequate in virtually all situations when nitrogen is addressed (irrespective of whether any modulated methodology is used or not), it is alternatively possible to rewrite it in a form that resembles the expressions previously given in the literature to express refractivity when the influences of the mirror penetration depth and the Gouy phase are neglected, as, for example, was done in the Refs. [35, 41, 42].[26] By defining an "effective" empty cavity frequency, ν_0', given by $\nu_0/(1+\frac{\Theta_G}{\pi m_0}+\frac{\gamma_s'}{m_0})$, it is possible to write

[26] Such an expression has often been written as

$$n-1=\frac{\overline{\Delta\nu}+\overline{\Delta q}}{1-\overline{\Delta\nu}+\varepsilon}, \tag{A.12}$$

Eq. (A.11) for working ranges not centred on the mirror center frequency in a more succinct form, viz. as

$$n-1=\frac{\overline{\Delta\nu}+\overline{\Delta m}}{1-\overline{\Delta\nu}+\frac{\Theta_G}{\pi m_0}+\varepsilon_0'}, \tag{A.13}$$

where $\overline{\Delta\nu}$ now is defined as $\overline{\Delta\nu}=\Delta\nu/\nu_0'$ and $\overline{\Delta m}$ is defined as $\frac{\Delta m}{m_0}$.

A comparison between the Eqs. (A.12) and (A.13) shows that the presence of mirror penetration depth and Gouy phase can be seen as a shift of the empty cavity laser frequency (transforming ν_0 to ν_0') and that the Gouy phase additionally provides a contribution in the denominator, similar to the distortion. In addition, it also shows that the relevant quantum number is m (as defined above) and not q (as used in the simplified expressions given in [35, 41, 42]), where the latter one is related to the former by $q=m+\frac{\Theta_G}{\pi}+n\gamma_s'$. This implies that also when the influences of the penetration depth and the Gouy phase are taken into account, it is possible to make use of the simplified expressions of the refractivity for which efficient evaluation procedures have been worked out when the GAMOR methodology is used, i.e. the Eq. (A.12), with a minimum of alterations (by shifting the empty cavity laser frequency from ν_0 to ν_0' and by interpreting ε as $\frac{\Theta_G}{\pi m_0}+\varepsilon_0'$ where ε_0' is defined as $\frac{\delta L}{L'}\frac{1}{n-1}$).

where $\overline{\Delta\nu}$ is defined as $\overline{\Delta\nu}=\Delta\nu/\nu_0$, $\overline{\Delta q}$ is a shorthand notation for $\Delta q/q_0$, where Δq is the number of mode jumps the measurement cavity laser has performed as a consequence of filling of the cavity while q_0 is the number of the mode addressed in the empty measurement cavity where the two q and q_0 mode numbers are defined through the relations $\nu=\frac{qc}{2n(L_0+\delta L)}$ and $\nu_0=\frac{q_0c}{2L_0}$, respectively, and where ε is defined as $\frac{\delta L}{L_0}\frac{1}{n-1}$.

B. Nomenclature and definitions of drifts

To assess the ability of GAMOR to reduce the influence of specific types of drifts, it has been found convenient to model the drift of the mode addressed in cavity i, i.e. $\nu_i^{(0)}(t)$, in terms of a Taylor series centered around the time instants at which each refractometry assessment is made (i.e. at t_g) as

$$\begin{aligned}\nu_i^{(0)}(t) = \nu_i^{(0)}(t_g) + \left(\frac{\partial \nu_i^{(0)}}{\partial t}\right)_{t_g}(t-t_g) + \\ \frac{1}{2}\left(\frac{\partial^2 \nu_i^{(0)}}{\partial t^2}\right)_{t_g}(t-t_g)^2 + ...,\end{aligned} \tag{B.1}$$

where $(\partial \nu_i^{(0)}/\partial t)_{t_g}$ and $(\partial^2 \nu_i^{(0)}/\partial^2 t)_{t_g}$ represent the amount of linear and first order non-linear drifts of the mode addressed in every modulation cycle, respectively.

Since the beat frequency is given by the difference in frequency of the two cavity modes addressed, for the case with empty cavities by $\nu_r^{(0)}(t) - \nu_m^{(0)}(t)$, this implies that there will be drifts also of the empty measurement cavity beat frequency, $f^{(0)}(t)$. Following the nomenclature above, this can be written as

$$\begin{aligned}f^{(0)}(t) = f^{(0)}(t_g) + \left(\frac{\partial f^{(0)}}{\partial t}\right)_{t_g}(t-t_g) + \\ \frac{1}{2}\left(\frac{\partial^2 f^{(0)}}{\partial t^2}\right)_{t_g}(t-t_g)^2 + ...,\end{aligned} \tag{B.2}$$

where

$$\begin{aligned}f^{(0)}(t_g) &= \nu_r^{(0)}(t_g) - \nu_m^{(0)}(t_g) \\ \left(\frac{\partial f^{(0)}}{\partial t}\right)_{t_g} &= \left(\frac{\partial \nu_r^{(0)}}{\partial t}\right)_{t_g} - \left(\frac{\partial \nu_m^{(0)}}{\partial t}\right)_{t_g} \\ \left(\frac{\partial^2 f^{(0)}}{\partial t^2}\right)_{t_g} &= \left(\frac{\partial^2 \nu_r^{(0)}}{\partial t^2}\right)_{t_g} - \left(\frac{\partial^2 \nu_m^{(0)}}{\partial t^2}\right)_{t_g}.\end{aligned} \tag{B.3}$$